

# Isogeometric de Rham complex discretization in solid toroidal domains

Francesco Patrizi

*Max-Planck-Institut für Plasmaphysik, Boltzmannstraße 2, 85748 Garching bei München, Germany*

---

## Abstract

In this work we define a spline complex preserving the cohomological structure of the continuous de Rham complex when the underlying physical domain is a toroidal solid. In the spirit of the *isogeometric analysis*, the spaces involved will be defined as pushforward of suitable spline spaces on a parametric domain. The singularity of the parametrization of the solid will demand the imposition of smoothness constraints on the full tensor product spline spaces in the parametric domain to properly set up the discrete complex on the physical domain.

*Keywords:* singularly parametrized domains, polar splines, numerical methods for electromagnetism.

---

## 1. Introduction

Isogeometric Analysis (IgA), introduced in [25], is a technique to perform numerical simulations on complicated geometries. As opposed to the Finite Elements Method (FEM), where the domain is approximated, usually by simplices, to allow the construction of numerical solutions in spaces of piecewise polynomials, the IgA approach gives priority to the geometric description of the problem. The numerical solution is then constituted by means of the functions used for the domain modeling. Nowadays, challenging geometries are usually expressed in terms of Computed Aided Design (CAD) shape functions, as B-splines, Non-Uniform Rational B-Splines (NURBS) and their generalization to address adaptive refineability [17, 32, 13, 19, 5, 14, 15].

The IgA approach has several advantages over FEM. Firstly, the geometry of the problem is exactly represented regardless of the fineness of the discretization. Secondly, while the numerical solution in FEM has  $C^0$  global continuity, in IgA the global smoothness of the approximation can be controlled by choosing meshline multiplicities and degrees. As a consequence, IgA improves the stability of the approximation (fewer nonphysical oscillations [25, 29]) and often it reaches a required accuracy using a much smaller number of degrees of freedom ( $\sim 90\%$  less, [20, 8]). Furthermore, the existing bottleneck in engineering is the creation of analysis suitable models from geometric models in CAD. This involves many steps that lead to the final domain approximation for FEM. This conversion is estimated to consume more than 80% of the overall analysis time. By adopting the IgA approach, all these conversion steps are not needed anymore and the model development is much faster and simplified.

In this paper we describe an IgA discretization for electromagnetics. For such physical phenomena, the reproduction of essential topological and homological structures at the discrete level is required to ensure accuracy and stability of the numerical method (see, e.g., [2, 3, 6, 23]). More precisely, we are interested in preserving the cohomological structure of the following de Rham complex:

$$0 \xrightarrow{\text{id}} H^1(\Omega^{pol}) \xrightarrow{\text{grad}} H(\text{curl}; \Omega^{pol}) \xrightarrow{\text{curl}} H(\text{div}; \Omega^{pol}) \xrightarrow{\text{div}} L^2(\Omega^{pol}) \xrightarrow{0} 0, \quad (1)$$

---

*Email address:* `francesco.patrizi@ipp.mpg.de` (Francesco Patrizi)

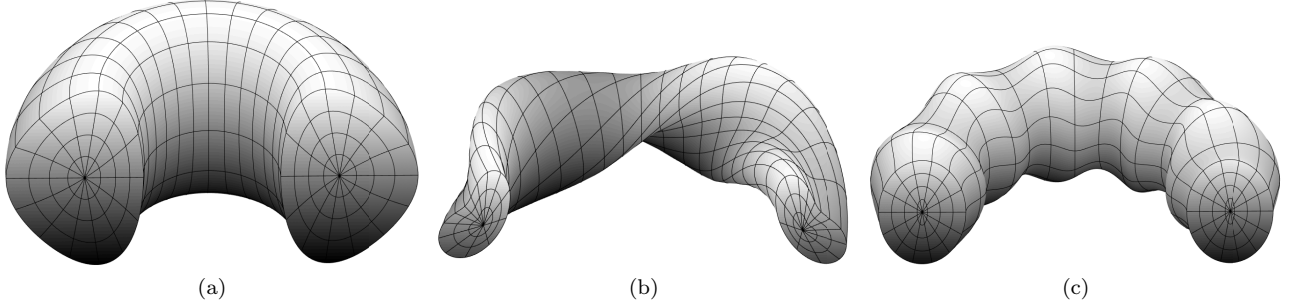


Figure 1: Simplified designs of half of the volumes inside the toroidal chambers of a tokamak (a) a stellarator (b) and a bumpy torus (c).

where

$$H(\text{curl}; \Omega^{pol}) = \{f \in (L^2(\Omega^{pol}))^3 \mid \text{curl } f \in (L^2(\Omega^{pol}))^3\},$$

$$H(\text{div}; \Omega^{pol}) = \{f \in (L^2(\Omega^{pol}))^3 \mid \text{div } f \in L^2(\Omega^{pol})\},$$

and  $\Omega^{pol}$  is a solid toroidal domain parametrized by a polar map. Such a map collapses a side of the parameter domain  $\Omega$  to a closed polar curve running around the hole of the toroidal domain. It is well known, see e.g. [21], that the dimension of the  $k$ th cohomology  $\mathcal{H}_{\text{dR}}^k$  of the de Rham complex (1) is equal to the  $k$ th Betti's number  $b_k$  of the domain. In our case, we have:

- $\dim \mathcal{H}_{\text{dR}}^0 = \dim \ker(\text{grad}) = b_0 = 1$ , the number of connected components forming  $\Omega^{pol}$ ,
- $\dim \mathcal{H}_{\text{dR}}^1 = \dim(\ker(\text{curl})/\text{im}(\text{grad})) = b_1 = 1$ , the number of “tunnels” in  $\Omega^{pol}$ ,
- $\dim \mathcal{H}_{\text{dR}}^2 = \dim(\ker(\text{div})/\text{im}(\text{curl})) = b_2 = 0$ , the number of voids enclosed in  $\Omega^{pol}$ ,
- $\dim \mathcal{H}_{\text{dR}}^3 = \dim(L^2(\Omega^{pol})/\text{im}(\text{div})) = b_3 = 0$ , by definition for any 3D domain.

The purpose of this work is to discretize the de Rham complex (1) in a spline complex on  $\Omega^{pol}$  preserving the above cohomology dimensions. The spline spaces involved in such discretization will be obtained by pushforward operators from spline spaces on the parametric domain  $\Omega$ . The singularity introduced by the polar map makes the standard tensor product spline spaces not suitable for this operation. In fact, the pushforward of the B-spline basis functions would be multivalued at the polar curve. As a consequence, the obtained discrete spaces on  $\Omega^{pol}$  would not be subspaces of the continuous counterparts in the de Rham complex (1). For this reason, we will define extraction operators leading to smoother restricted spaces, in the tensor product spline spaces on  $\Omega$ , for which the pushforward operators can be applied to obtain appropriate approximant spaces of  $H^1(\Omega^{pol})$ ,  $H(\text{curl}; \Omega^{pol})$ ,  $H(\text{div}; \Omega^{pol})$  and  $L^2(\Omega^{pol})$  forming, moreover, a spline complex preserving the cohomological structure of (1).

We are interested in toroidal domains because these geometries are of particular relevance in the problem of controlled thermonuclear reactions, especially in fusion reactors based on magnetic confinements. In these devices, plasma is confined by the magnetic fields created by a fixed set of external current-carrying conductors located at the boundary walls. In order to prevent dramatically losses of energy and plasma density, the magnetic field lines should not intersect such conductors or even the vacuum chamber located between plasma and material walls. The study of ideal magnetic hydrodynamics equilibria leads to relatively complicated toroidal geometries, such as tokamaks, stellarators and bumpy tori, see Figure 1, which can be employed to confine and isolate plasma from material walls and keep it stable for relatively large values of the ratio energy produced/energy used. Further details can be found, e.g., in the books [18] and [22]. Numerical methods for the simulation of magnetically confined plasma have been studied and developed since the early '60s. Nevertheless, only recently spline spaces for grid-based discretizations have been adopted, see, e.g., [4, 27, 24, 39, 12]. Such numerical models rely on the approximations of electromagnetic fields in the IgA framework built using tensor-product splines [10, 9] and, more recently, adaptively-refined splines [11, 26, 16].

However, the establishing of plasma simulations within physical domains parametrized by means of polar maps still constitute a major difficulty, due to the singularity introduced at the polar curves. In [39] a model providing a  $C^1$  continuous approximation is proposed on a 2D disk-like domain using the so called *polar splines* [36, 34]. Polar splines have also been used for the discretization of the 2D de Rham complex on a disk-like domain [35]. This work can indeed be reckoned as an extension of [35] to a 3D solid toroidal domain. However, as opposed to it, we have chosen to use the standard functional analysis terminology instead of introducing the more abstract, but perhaps more elegant, formalism of the finite element exterior calculus, for the sake of brevity and concreteness.

The next sections are organized as follows. In Section 2 we first introduce the notations used in this paper and recall some basic concepts of the spline theory. Then we set the framework for our construction and we provide an overview of the desired discretization by means of a diagram. In Section 3 we define the extraction operators and the restricted spline spaces employed in the parametric domain for the construction of the spline complex on the physical domain. In Section 4 we prove the preservation of the cohomological structure of (1) at the discrete level and in Section 5 we draw the conclusions.

## 2. Preliminaries & discretization overview

In this section we present the framework and tools we need for the discretization. We further picture the process in a diagram created from the de Rham complex (1). In this paper we have chosen to set it up with spline spaces generated by B-splines for the sake of simplicity and brevity. However, an analogous construction could be done starting from, e.g., *multi-degree spline spaces* (see [36, 37, 33, 34]), i.e., collections of NURBS spaces (of different degrees and weights) glued together with some prescribed smoothness.

We assume the reader to be familiar with the definition and main properties of B-splines. An introduction to this topic can be found, e.g., in the review papers [28, 30] or in the classical books [7] and [31]. What follows only introduces the notations adopted in this work.

### 2.1. Preliminaries

Given a degree  $p \geq 0$  and an open knot vector  $\mathbf{t} = (t_1, \dots, t_{n+p+1}) \subset \mathbb{R}$ , we indicate as  $B_j^p$  the  $j$ th B-spline of degree  $p$  defined on  $\mathbf{t}$ . The spline space generated by all the B-splines of degree  $p$  on  $\mathbf{t}$  will be denoted as  $\mathbb{S}_{\mathbf{t}}^p = \text{span} \{B_j^p\}_{j=1}^n$ . A spline space  $\mathbb{S}_{\mathbf{t}}^p$  is  $C^k$ , for  $k \geq 0$ , if its elements have global smoothness greater or equal to  $C^k$  in the interval spanned by the knot vector. Given a  $C^k$  spline space  $\mathbb{S}_{\mathbf{t}}^p$ , we define its **periodic subspace**,  $\mathbb{S}_{\mathbf{t}, \circlearrowleft}^p$ , as the space of splines  $f \in \mathbb{S}_{\mathbf{t}}^p$  which further satisfy

$$f^{(j)}(t_1) = f^{(j)}(t_{n+p+1}) \quad \text{for } j = 0, \dots, k.$$

For  $C^1$  spaces, if  $\mathbf{B}^{(0)}$  is the vector containing the B-splines spanning  $\mathbb{S}_{\mathbf{t}}^p$  arranged following the supports ordering on the real line, then  $\mathbb{S}_{\mathbf{t}, \circlearrowleft}^p$  is spanned by the functions contained in the vector

$$\mathbf{B}_{\circlearrowleft}^{(0)} := H^{(0)} \mathbf{B}^{(0)} \tag{2}$$

where  $H^{(0)}$  is the rectangular matrix of size  $(n-2) \times n$  defined as  $H^{(0)} = [\mathbf{c} | I_{n-2} | \mathbf{c}]$  with  $I_{n-2}$  the identity matrix of size  $n-2$  and

$$\mathbf{c} = \begin{bmatrix} c_1 \\ 0 \\ \vdots \\ 0 \\ c_2 \end{bmatrix} \quad \text{for } (c_1, c_2) = \frac{(t_{n+p+1} - t_n, t_{p+2} - t_1)}{t_{n+p+1} - t_n + t_{p+2} - t_1}.$$

The construction and understanding of matrix  $H^{(0)}$  is detailed in the setting of multi-degree splines in [34]. A more general assemble algorithm, for  $C^k$  periodicity with any  $k \geq 0$ , is illustrated in [36, 33]. Figure 2

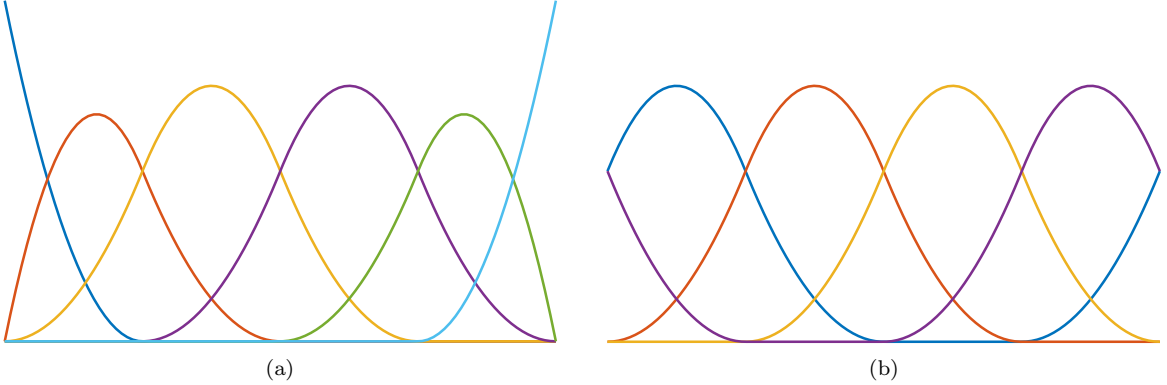


Figure 2: The B-spline basis of the quadratic  $C^1$  spline space (a) and the basis functions of the quadratic  $C^1$  periodic spline space (b) on the uniform open knot vector of five distinct knots  $\mathbf{t} = [0, 0, 0, 1, 2, 3, 4, 4, 4]$ . We stress that the basis functions in (b) tie in at the endpoints of the interval with  $C^1$  continuity.

visually compares the B-spline basis of  $\mathbb{S}_{\mathbf{t}}^p$  with the basis functions of  $\mathbb{S}_{\mathbf{t},\mathcal{O}}^p$ , for  $p = 2$  and  $\mathbf{t}$  an uniform open knot vector with five distinct knots. Note that the first and last basis functions in  $\mathbf{B}_{\mathcal{O}}^{(0)}$  are not B-splines. However they preserve all the B-spline properties when identifying the endpoints of the interval. Therefore we will not stress this fact again and, with an abuse of terminology for the sake of simplicity, we will call them B-splines as well and use the same notation.

A useful relation we will make large use of is the **derivative formula for splines**. Let  $\mathbb{S}_{\mathbf{t}}^p = \text{span} \{B_j^p\}_{j=1}^n$  be a  $C^1$  spline space. Given  $f \in \mathbb{S}_{\mathbf{t}}^p$ ,

$$f(t) = \sum_{j=1}^n f_j B_j^p(t)$$

we have that

$$f'(t) = \sum_{j=1}^{n-1} (f_{j+1} - f_j) D_j^p(t) \quad \text{where } D_j^p(t) = \frac{p}{t_{j+p+1} - t_{j+1}} B_{j+1}^{p-1}(t), \quad (3)$$

with the  $B_j^{p-1}$  defined on the knot vector  $\hat{\mathbf{t}} = (\hat{t}_1, \dots, \hat{t}_{n+p-1}) = (t_2, \dots, t_{n+p}) \subset \mathbf{t}$  for all  $j$ . Let again  $\mathbf{B}^{(0)}$  be the vector of the B-spline basis  $\{B_j^p\}_{j=1}^n$ . If  $\mathbf{f}$  is the vector of coefficients  $(f_1, \dots, f_n)^T$ , then  $f = \mathbf{B}^{(0)} \cdot \mathbf{f}$  and the derivative formula (3) can be written as a matrix expression:

$$f'(t) = \mathbf{B}^{(1)} \cdot \mathfrak{D}_n \mathbf{f} \quad (4)$$

where  $\mathbf{B}^{(1)}$  is the vector of functions  $\{D_j^p\}_{j=1}^{n-1}$  and  $\mathfrak{D}_n$  the following rectangular matrix of size  $(n-1) \times n$

$$\mathfrak{D}_n = \begin{bmatrix} -1 & 1 & & & \\ & \ddots & \ddots & \mathbb{O} & \\ & & \ddots & \ddots & \\ \mathbb{O} & & & & \\ & & & -1 & 1 \end{bmatrix}. \quad (5)$$

The span of the functions in  $\mathbf{B}^{(1)}$  is the  $C^0$  spline space  $\mathbb{S}_{\mathbf{t}}^{p-1}$  (see, e.g., [28, Theorems 6–7]).

In the periodic spline space a derivative formula similar to Equation (4) holds true. Let  $\mathbb{S}_{\mathbf{t},\mathcal{O}}^p$  be the  $C^1$  periodic spline space spanned by the functions in the vector  $\mathbf{B}_{\mathcal{O}}^{(0)}$ . Then a spline  $f_{\mathcal{O}} \in \mathbb{S}_{\mathbf{t},\mathcal{O}}^p$  can be expressed as  $f_{\mathcal{O}} = \mathbf{B}_{\mathcal{O}}^{(0)} \cdot \mathbf{f}_{\mathcal{O}}$  for a vector of coefficients  $\mathbf{f}_{\mathcal{O}}$ . The derivative of  $f_{\mathcal{O}}$  is

$$f'_{\mathcal{O}}(t) = \mathbf{B}_{\mathcal{O}}^{(1)} \cdot \mathfrak{D}_{n-2,\mathcal{O}} \mathbf{f}_{\mathcal{O}}$$

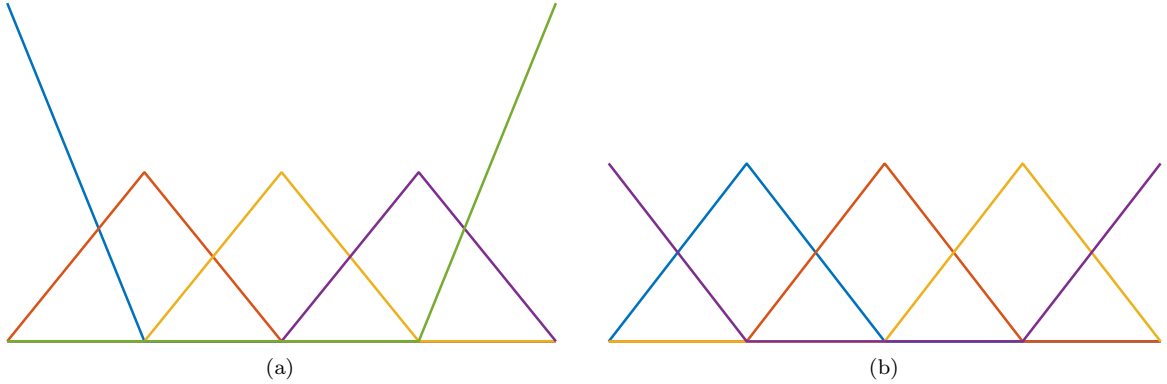


Figure 3: Comparison of the linear spline functions spanning the derivatives of the quadratic splines generated by the bases reported in Figure 2 (a)-(b) respectively. These derivatives are  $C^0$  (a) and  $C^0$  periodic (b) respectively as the linear splines in (b) tie in at the endpoints of the interval with  $C^0$  continuity.

where  $\mathfrak{D}_{n-2,\mathcal{O}}$  is the square matrix of size  $n - 2$

$$\mathfrak{D}_{n-2,\mathcal{O}} = \begin{bmatrix} -1 & 1 & & & & \\ & \ddots & \ddots & & & \mathcal{O} \\ & & \mathcal{O} & \ddots & \ddots & \\ & & & & & -1 & 1 \\ 1 & 0 & \cdots & 0 & -1 & \end{bmatrix}, \quad (6)$$

and  $\mathbf{B}_{\mathcal{O}}^{(1)}$  is a vector of splines  $\{D_{j,\mathcal{O}}^p\}_{j=1}^{n-2}$  spanning the  $C^0$  periodic space  $\mathbb{S}_{\mathcal{O}}^{p-1}$  given by

$$\mathbf{B}_{\mathcal{O}}^{(1)} = H^{(1)} \mathbf{B}^{(1)} \quad (7)$$

where  $H^{(1)}$  is the following rectangular matrix of size  $(n - 2) \times (n - 1)$ :

$$H^{(1)} = \left[ \begin{array}{c|cc|c} 0 & & & 0 \\ \vdots & I_{n-3} & & \vdots \\ \vdots & & & \vdots \\ 0 & & & 0 \\ \hline c_2 & 0 & \cdots & 0 & c_1 \end{array} \right].$$

with  $I_{n-3}$  the identity matrix of size  $n - 3$ . In Figure 3 we visually compare the functions in  $\mathbf{B}^{(1)}$  and  $\mathbf{B}_{\mathcal{O}}^{(1)}$  when  $\mathbf{B}^{(0)}$  and  $\mathbf{B}_{\mathcal{O}}^{(0)}$  contain the splines in Figure 2 (a)-(b) respectively.

Another notion we need is the definition of **design-through-analysis compatible matrix**, introduced in [34]. Consider a set of B-spline like functions, that is, a set of functions that are linearly independent, locally supported and that form a positive partition of unity. When a design-through-analysis compatible, or DTA-compatible, matrix is applied to such a collection, it provides another set of B-spline like functions. More precisely, a matrix  $E$  is DTA-compatible, if

- $E$  has full rank (preservation of the linear independence),
- each column of  $E$  sums to 1 (preservation of the partition of unity),
- each entry of  $E$  is non-negative (preservation of the positivity),

- $E$  preserves the locality of the supports through sparsity.

We have already seen an example of such matrices (aside the identity matrix). The matrix  $H^{(0)}$  of Equation (2), which transforms the B-spline basis of  $\mathbb{S}_t^p$  in the basis of  $\mathbb{S}_{t,\Omega}^p$  is a DTA-compatible matrix.

Finally, we make the following simple remark which, nevertheless, will be fundamental to prove commutation in the discretization diagram.

**Remark 2.1.** *Let  $A$  be a functional vector space spanned by  $\{\alpha_j\}_{j=1}^n$  and let  $B \subseteq A$  be a subspace spanned by  $\{\beta_i\}_{i=1}^m$ . If the vectors  $\boldsymbol{\alpha}$  and  $\boldsymbol{\beta}$  contain the bases of  $A$  and  $B$  respectively, let  $M = (m_{ij})_{i,j=1}^{m,n}$  be the restriction matrix,  $\boldsymbol{\beta} = M\boldsymbol{\alpha}$ . Let  $f \in B$ ,  $f = \sum_{i=1}^m b_i \beta_i$  for  $\{b_i\}_{i=1}^m \subset \mathbb{R}$ . We can always write  $f$  in terms of the basis functions of  $A$ ,  $\{\alpha_j\}_{j=1}^n$ :*

$$f = \sum_{i=1}^m b_i \beta_i = \sum_{i=1}^m \sum_{j=1}^n b_i m_{ij} \alpha_j = \sum_{j=1}^n a_j \alpha_j,$$

where the coefficients  $\{a_j\}_{j=1}^n$  are defined as

$$a_j = \sum_{i=1}^m b_i m_{ij} \quad \forall j = 1, \dots, n.$$

In other words, the relation between the coefficients to express  $f$  in the basis of  $A$  is  $\boldsymbol{a} = M^T \boldsymbol{b}$  with  $\boldsymbol{a} = (a_1, \dots, a_n)^T$  and  $\boldsymbol{b} = (b_1, \dots, b_m)^T$ .

## 2.2. Problem setting & discretization overview

We now present the discretization of the de Rham complex (1) that leads to a spline complex preserving the cohomology dimensions, in a solid toroidal domain  $\Omega^{pol}$ , by means of a diagram. We shall prove that such diagram commutes.

For the sake of simplicity, we drop the subscripts in the spline spaces we are going to define hereafter, as their specific knot vectors will be not relevant anymore and their possible periodicity will be clear from the context.

Given a multidegree  $\mathbf{p} = (p^r, p^s, p^t)$ , let

- $\mathbb{S}^{p^r}$  be a  $C^1$  periodic spline space defined on the interval  $[0, R] \subset \mathbb{R}$  spanned by the B-splines  $\{B_i^{p^r}\}_{i=1}^{n^r}$ ,
- $\mathbb{S}^{p^s}$  be a  $C^1$  spline space defined on the interval  $[0, S] \subseteq \mathbb{R}$  spanned by the B-splines  $\{B_j^{p^s}\}_{j=1}^{n^s}$ ,
- $\mathbb{S}^{p^t}$  be a  $C^1$  periodic spline space defined on the interval  $[0, T] \subseteq \mathbb{R}$  spanned by the B-splines  $\{B_k^{p^t}\}_{k=1}^{n^t}$ .

We define the **parameter domain**  $\Omega$  as the Cartesian product of the intervals,  $\Omega := [0, R] \times [0, S] \times [0, T]$ , and the **spline space in  $\Omega$** ,  $\mathbb{S}^{p^r, p^s, p^t}$ , as the tensor product of the univariate spline spaces on such intervals:

$$\mathbb{S}^{p^r, p^s, p^t} := \mathbb{S}^{p^r} \otimes \mathbb{S}^{p^s} \otimes \mathbb{S}^{p^t} = \text{span} \{B_{ijk}^{\mathbf{p}} := B_i^{p^r} B_j^{p^s} B_k^{p^t}\}_{i,j,k=1}^{n^r, n^s, n^t}.$$

Let  $F : \Omega \rightarrow \Omega^{pol}$  be the **polar map**,

$$\Omega \ni (r, s, t) \mapsto F(r, s, t) = (F_u(r, s, t), F_v(r, s, t), F_w(r, s, t)) = (u, v, w) \in \Omega^{pol},$$

which transforms  $\Omega$  into the toroidal domain  $\Omega^{pol}$ , see Figure 4. We assume  $F$  in the spline space  $\mathbb{S}^{p^r, p^s, p^t}$ , that is,

$$F(r, s, t) := \sum_{k=1}^{n^t} \sum_{j=1}^{n^s} \sum_{i=1}^{n^r} \mathbf{F}_{ijk} B_{ijk}^{\mathbf{p}}(r, s, t)$$

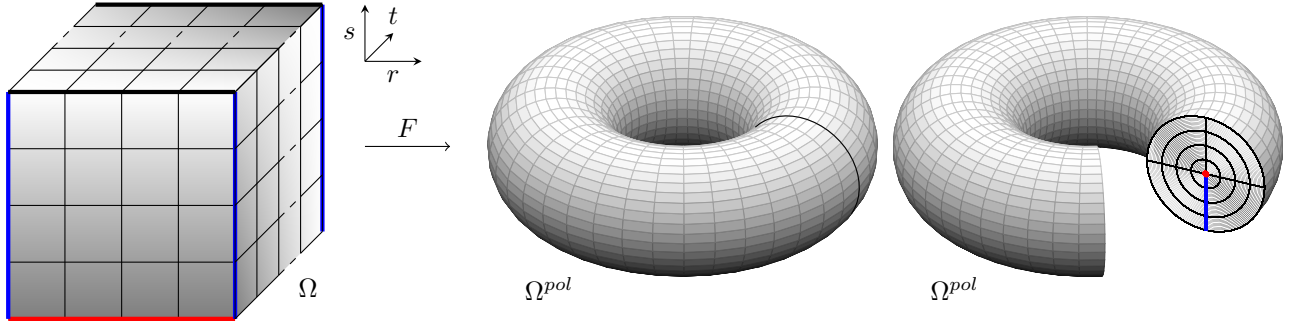


Figure 4: The transformation of the parametric domain  $\Omega$  into the toroidal domain  $\Omega^{pol}$  by the polar map  $F$ . The three-dimensional tensor mesh defined on  $\Omega$  is mapped to a three-dimensional polar mesh in  $\Omega^{pol}$ . The latter can be seen in the right-most figure.

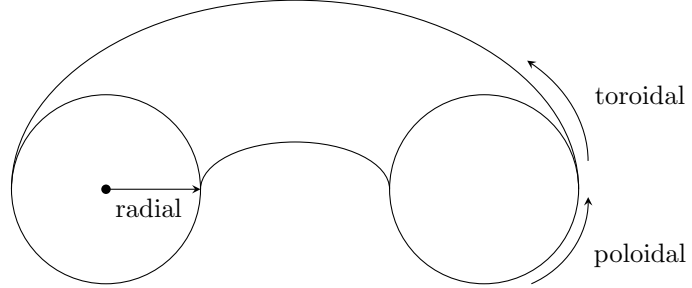
with  $\mathbf{F}_{ijk} = ((\bar{\rho} + \rho_j \cos \theta_i) \cos \varphi_k, (\bar{\rho} + \rho_j \cos \theta_i) \sin \varphi_k, \rho_j \sin \theta_i)^T \in \mathbb{R}^3$ , for  $\bar{\rho} > 2$  a fixed number and

$$\rho_j = \frac{j-1}{n^s-1} \in [0, 1] \quad \text{for } j = 1, \dots, n^s,$$

$$\theta_i = 2\pi + \frac{(1-2i)\pi}{n^r} \in [0, 2\pi] \quad \text{for } i = 1, \dots, n^r,$$

$$\varphi_k = 2\pi + \frac{(1-2k)\pi}{n^t} \in [0, 2\pi] \quad \text{for } k = 1, \dots, n^t.$$

With reference to Figure 4, the map  $F$  identifies in  $\Omega^{pol}$  the left side with the right side and the front side with the back side of  $\Omega$ . The bottom side is instead collapsed to a **polar curve** running around the hole of  $\Omega^{pol}$ . Let us introduce the following **radial, toroidal and poloidal directions** in  $\Omega^{pol}$ :



with the radial direction generating from the polar curve. We further define the **pushforward B-splines** as the images via  $F$  of the B-splines spanning  $\mathbb{S}^{p^r, p^s, p^t}$ , i.e., the collection of functions  $B_{ijk}^{\mathbf{p}, pol} : \Omega^{pol} \rightarrow \mathbb{R}$  defined as

$$B_{ijk}^{\mathbf{p}, pol} := B_{ijk}^{\mathbf{p}} \circ F^{-1} \quad \forall i, j, k.$$

Except at the polar curve, where  $F^{-1}$  is not well-defined and the pushforward B-splines are multivalued, the  $B_{ijk}^{\mathbf{p}, pol}$  are  $C^1$ -continuous in the radial direction. Such smoothness is drawn from the basis elements in  $\mathbb{S}^{p^s}$ . In the same way and thanks to the periodicity of the univariate spline spaces  $\mathbb{S}^{p^t}$  and  $\mathbb{S}^{p^r}$ , the  $C^1$ -continuity of the pushforward B-splines is also guaranteed in the toroidal and poloidal directions, far from the polar curve. However, our strategy for the discretization of the de Rham complex (1) is to construct a space  $V_0^{pol} \subseteq H^1(\Omega^{pol})$  of splines which are  $C^1$ -differentiable in  $\Omega^{pol}$ , in particular at the polar curve, and then look for spline spaces  $V_1^{pol}, V_2^{pol}, V_3^{pol}$ , in  $H(\text{curl}; \Omega^{pol}), H(\text{div}; \Omega^{pol})$  and  $L^2(\Omega^{pol})$  respectively, such that the differential operators “grad”, “curl” and “div” are locally exact near the polar curve. In this manner, every element of  $V_1^{pol}$  would be the gradient of an element in  $V_0^{pol}$ , every element of  $V_2^{pol}$  would be the curl of an element in  $V_1^{pol}$  and every element of  $V_3^{pol}$  would be the divergence of an element in  $V_2^{pol}$ , near the

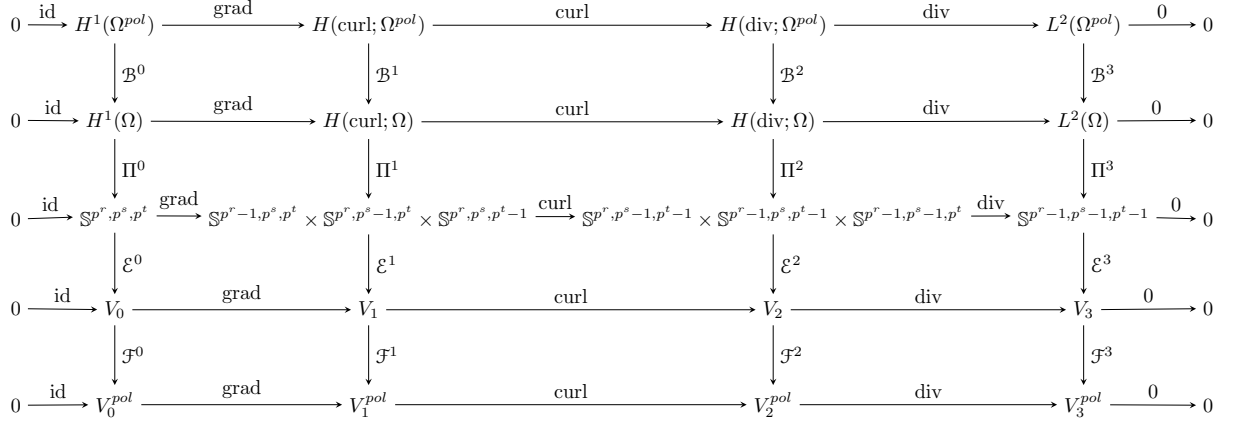


Figure 5: The scheme of the full discretization process that leads to a spline complex on  $\Omega^{pol}$  (bottom row) from the de Rham complex (1) (top row), preserving the cohomological structure of the latter. The three intermediate rows are complexes on the parameter domain  $\Omega$ .

polar curve in  $\Omega^{pol}$ . As a consequence, the  $C^1$ -smoothness in  $V_0^{pol}$  would ensure the  $C^0$ -smoothness of the functions in  $V_1^{pol}$  and  $V_2^{pol}$  and the boundness of the elements of  $V_3^{pol}$ , despite the global  $C^{-1}$ -continuity. For this reason, an extraction operation to reduce the spline space to a suitable subspace where  $F$  is invertible is required.

All the spaces  $V_0^{pol}, V_1^{pol}, V_2^{pol}$  and  $V_3^{pol}$  will be obtained by pushforward operators from reduced spline spaces on the parameter domain  $\Omega$ . The full discretization process is schematized in the diagram of Figure 5. The first row is the de Rham complex (1). The operators  $\mathcal{B}^i$  are the **pullback operators** and are defined as

$$\begin{aligned}
H^1(\Omega^{pol}) &\ni \phi^{pol} \mapsto \mathcal{B}^0(\phi^{pol}) := \phi \circ F =: \phi \in H^1(\Omega), \\
H(\text{curl}; \Omega^{pol}) &\ni \phi^{pol} \mapsto \mathcal{B}^1(\phi^{pol}) := (DF)^T(\phi \circ F) =: \phi \in H(\text{curl}; \Omega), \\
H(\text{div}; \Omega^{pol}) &\ni \phi^{pol} \mapsto \mathcal{B}^2(\phi^{pol}) := \det(DF)(DF)^{-1}(\phi \circ F) =: \phi \in H(\text{div}; \Omega), \\
L^2(\Omega^{pol}) &\ni \phi^{pol} \mapsto \mathcal{B}^3(\phi^{pol}) := \det(DF)(\phi \circ F) =: \phi \in L^2(\Omega),
\end{aligned}$$

where  $DF$  is the Jacobian matrix of  $F$ .

The operators  $\Pi^0, \Pi^1, \Pi^2$  and  $\Pi^3$  are **projectors** which discretize the continuous de Rham complex in  $\Omega$  by means of tensor product spline spaces. Their definitions and the proof of commutation of the subdiagram composed by the first three rows are contained in [9].

At this stage we have a discrete complex on the parametric domain  $\Omega$  using tensor product spline spaces. As we have already pointed out, in order to move back onto the physical domain  $\Omega^{pol}$ , we first have to extract reduced spline spaces  $V_0, V_1, V_2$  and  $V_3$  on  $\Omega$  in which we can apply the pushforward operators. The extraction operators  $\mathcal{E}^0, \mathcal{E}^1, \mathcal{E}^2$  and  $\mathcal{E}^3$  and the definition of such spaces are the content of Section 3. The **pushforward operators**  $\mathcal{F}^0, \mathcal{F}^1, \mathcal{F}^2, \mathcal{F}^3$  can finally be employed to obtain our final discretization on  $\Omega^{pol}$ .

These are defined as the inverses of the pullback operators,  $\mathcal{F}^\ell := (\mathcal{B}^\ell)^{-1}$  for  $\ell = 0, \dots, 3$ , that is:

$$\begin{aligned}
V_0 \ni \phi &\mapsto \mathcal{F}^0(\phi) := \phi \circ F^{-1} =: \phi^{pol} \in V_0^{pol}, \\
V_1 \ni \phi &\mapsto \mathcal{F}^1(\phi) := (DF^{-T}\phi) \circ F^{-1} =: \phi^{pol} \in V_1^{pol}, \\
V_2 \ni \phi &\mapsto \mathcal{F}^2(\phi) := ((\det DF)^{-1}DF\phi) \circ F^{-1} =: \phi^{pol} \in V_2^{pol}, \\
V_3 \ni \phi &\mapsto \mathcal{F}^3(\phi) := ((\det DF)^{-1}\phi) \circ F^{-1} =: \phi^{pol} \in V_3^{pol}.
\end{aligned} \tag{8}$$

The space  $V_0^{pol}$  in the definition of  $\mathcal{F}^0$  is referred to as **polar spline space** in the literature [36, 34, 35]. We shall show that the discretization process is well-defined by proving commutation of the diagram and we shall verify that the spline complex at the last row of the diagram preserves the cohomology dimensions of the continuous de Rham complex at the first row.

### 3. Extraction operators and reduced spaces in $\Omega$

In this section we identify subspaces of the full tensor product spline spaces in the parameter domain, for which the pushforward operators can be applied in order to create appropriate approximant spaces for  $H^1(\Omega^{pol})$ ,  $H(\text{curl}; \Omega^{pol})$ ,  $H(\text{div}; \Omega^{pol})$  and  $L^2(\Omega^{pol})$ . Extraction operators will be defined to determine such reduced spline spaces. We further show the commutation of such extraction operators with the differential operators grad, curl and div.

#### 3.1. The operator $\mathcal{E}^0$ and the space $V_0$

Let  $f \in \mathbb{S}^{p^r, p^s, p^t}$  and  $f^{pol} := \mathcal{F}^0(f)$  be the corresponding pushforward spline on  $\Omega^{pol}$ , that is,

$$f(r, s, t) = f^{pol}(F(r, s, t)).$$

We have that  $f^{pol} \in C^1(\Omega^{pol})$  if  $f^{pol}$  is well-defined and  $C^1$  in the radial, poloidal and toroidal directions everywhere in  $\Omega^{pol}$ . The polar map  $F$  collapses the bottom side of  $\Omega$ ,  $\{(r, s, t) \in \Omega \mid s = 0\}$ , to a polar curve lying on the plane  $\{(u, v, w) \in \mathbb{R}^3 \mid w = 0\}$ . Indeed, by using the fact that only  $B_1^{p^s}(0) \neq 0$  and that the sum over the  $B_i^{p^r}(r)$  is one for any  $r \in [0, R]$ , we have

$$\begin{aligned}
F(r, 0, t) &= \sum_{k=1}^{n^t} \sum_{j=1}^{n^s} \sum_{i=1}^{n^r} ((\bar{\rho} + \rho_j \cos \theta_i) \cos \varphi_k, (\bar{\rho} + \rho_j \cos \theta_i) \sin \varphi_k, \rho_j \sin \theta_i)^T B_i^{p^r}(r) B_j^{p^s}(s) B_k^{p^t}(t) \\
&= \sum_{k=1}^{n^t} \sum_{i=1}^{n^r} (\bar{\rho} \cos \varphi_k, \bar{\rho} \sin \varphi_k, 0)^T B_i^{p^r}(r) B_k^{p^t}(t) \quad (\text{because } B_1^{p^s}(0) = 1) \\
&= \sum_{k=1}^{n^t} (\bar{\rho} \cos \varphi_k, \bar{\rho} \sin \varphi_k, 0)^T B_k^{p^t}(t).
\end{aligned}$$

Thus, by imposing that  $f(r, 0, t)$  is constant in the  $r$  direction, that is

$$f(r, 0, t) \in \mathbb{S}^{p^t}, f(r, 0, t) = \sum_{k=1}^{n^t} \alpha_k B_k^{p^t}(t), \tag{9}$$

with  $\alpha_k \in \mathbb{R}$  for  $k = 1, \dots, n^t$ , we ensure that  $f^{pol}$  is well-defined and that its restriction to the toroidal direction is  $C^1$ -continuous in  $\Omega^{pol}$ , as  $\mathbb{S}^{p^t}$  is  $C^1$  periodic.

The conditions to have  $f^{pol}$   $C^1$ -smooth also in the radial and poloidal directions have been analyzed in [34]. These enforce the following further relation to be satisfied together with Equation (9): there must exist  $\beta_k, \gamma_k \in \mathbb{R}$  for  $k = 1, \dots, n^t$  such that

$$\frac{\partial}{\partial s} f(r, 0, t) = \sum_{k=1}^{n^t} \sum_{j=1}^2 \sum_{i=1}^{n^r} [\mathbf{F}_{ijk} \cdot (\beta_k, \gamma_k)] \frac{\partial}{\partial s} B_{ijk}(r, 0, t), \quad (10)$$

with  $\mathbf{F}_{ijk}$  the control points of the polar map. By following the construction of [34], we have that Equations (9)-(10) are verified if  $f$  is taken in the restricted space  $V_0$ , which is defined via an extraction operator  $\mathcal{E}^0 : \mathbb{S}^{p^r, p^s, p^t} \rightarrow V_0$  as follows. Let  $\mathbf{B}^{(0,0,0)}$  be the vectorization of the B-spline basis  $\{B_{ijk}^{\mathbf{p}}\}_{i,j,k=1}^{n^r, n^s, n^t}$  of  $\mathbb{S}^{p^r, p^s, p^t}$ , that is,  $B_{i+(j-1)n^r+(k-1)n^s}^{(0,0,0)} := B_{ijk}^{\mathbf{p}}$  for any  $i, j, k$ . Then  $V_0$  is spanned by the splines in the collection  $\mathbf{N}^{(0)}$  given by

$$\mathbf{N}^{(0)} = E^{(0,0,0)} \mathbf{B}^{(0,0,0)} \quad (11)$$

where  $E^{(0,0,0)}$  is the restriction matrix, of size  $n^t(n^r(n^s - 2) + 3) \times n^r n^s n^t$ , associated to  $\mathcal{E}^0$ .  $E^{(0,0,0)}$  is defined as  $E^{(0,0,0)} = I_{n^t} \otimes E^{(0)}$  with  $I_{n^t}$  the identity matrix of size  $n^t$  and  $E^{(0)}$  the following block matrix, introduced in [36]:

$$E^{(0)} = \begin{bmatrix} \bar{E} & \circ \\ \circ & I_{n^r(n^s-2)} \end{bmatrix}, \quad \bar{E} = \begin{bmatrix} \bar{E}_{1,(1,1)} & \cdots & \bar{E}_{1,(n^r,1)} & \bar{E}_{1,(1,2)} & \cdots & \bar{E}_{1,(n^r,2)} \\ \bar{E}_{2,(1,1)} & \cdots & \bar{E}_{2,(n^r,1)} & \bar{E}_{2,(1,2)} & \cdots & \bar{E}_{2,(n^r,2)} \\ \bar{E}_{3,(1,1)} & \cdots & \bar{E}_{3,(n^r,1)} & \bar{E}_{3,(1,2)} & \cdots & \bar{E}_{3,(n^r,2)} \end{bmatrix} \quad (12)$$

where  $I_{n^r(n^s-2)}$  is the identity matrix of size  $n^r(n^s - 2)$  and  $\bar{E}$  the rectangular matrix of size  $3 \times 2n^r$  whose elements are:

$$\bar{E}_{\ell,(i,1)} = \frac{1}{3} \quad \forall \ell = 1, 2, 3 \text{ and } \forall i = 1, \dots, n^r,$$

$$\begin{bmatrix} \bar{E}_{1,(i,2)} \\ \bar{E}_{2,(i,2)} \\ \bar{E}_{3,(i,2)} \end{bmatrix} = \begin{bmatrix} \frac{1}{3} \\ \frac{1}{3} \\ \frac{1}{3} \end{bmatrix} + \begin{bmatrix} \frac{1}{3} & 0 \\ -\frac{1}{6} & \frac{\sqrt{3}}{6} \\ -\frac{1}{6} & -\frac{\sqrt{3}}{6} \end{bmatrix} \begin{bmatrix} \cos \theta_i \\ \sin \theta_i \end{bmatrix} \quad \forall i = 1, \dots, n^r.$$

As  $E^{(0)}$  is DTA-compatible [34, Theorem 3.2], also  $E^{(0,0,0)}$  is DTA-compatible. This means that the functions in  $\mathbf{N}^{(0)}$ ,  $\{N_{\ell}^{(0)}\}_{\ell=1}^{n_0}$  with  $n_0 := n^t(n^r(n^s - 2) + 3)$ , are linearly independent, locally supported and form a convex partition of unity on  $\Omega$ . Moreover their pushforward counterpart,  $N_{\ell}^{(0),pol} : \Omega^{pol} \rightarrow \mathbb{R}$ , defined as

$$N_{\ell}^{(0),pol} := \mathcal{F}^0(N_{\ell}^{(0)}) = N_{\ell}^{(0)} \circ F^{-1},$$

are well-defined,  $C^1$ -smooth, linearly independent and form a convex partition of unity on  $\Omega^{pol}$ .

### 3.2. Geometric interpretation of the degrees of freedom

A geometric interpretation to the degrees of freedom (DOFs) defining the functions in  $\mathbb{S}^{p^r, p^s, p^t}$ ,  $V_0$  and in the spaces we are going to consider in the next sections will help us understand the action of the differential operators on such discrete spaces and will make the discretization scheme reported in Figure 5 clearer. This interpretation was introduced in [11] and adopted later in, e.g., [16, 35]. Suppose to have a spline complex on the parameter domain  $\Omega$ :

$$\mathfrak{X} : \quad 0 \xrightarrow{\text{id}} X_0 \xrightarrow{\text{grad}} X_1 \xrightarrow{\text{curl}} X_2 \xrightarrow{\text{div}} X_3 \xrightarrow{0} 0.$$

$X_0$  could be, for instance, the full spline space  $\mathbb{S}^{p^r, p^s, p^t}$  or the restricted space  $V_0$ . Suppose also to have a geometry map  $G : \Omega \rightarrow \Omega^G$ , from the parameter domain  $\Omega$  to some physical domain  $\Omega^G$  and let  $G$  belong to  $X_0$ . From  $G$  one can define the control mesh  $\mathcal{M}^G$  by connecting its control points. Finally, let us assume

the pushforward operators for  $G$  with respect to  $\mathfrak{X}$ ,  $\mathcal{G}_\ell$  with  $\ell = 0, 1, 2, 3$ , to be well defined. Then [11, Proposition 4.4] ensures that the spline complex  $\mathfrak{X}$  is isomorphic to the **cochain complex on  $\mathcal{M}^G$** . The latter can be defined modifying the definition of simplicial cochain complexes [1, Section 2.5] by replacing the underlying triangulation with the control mesh  $\mathcal{M}^G$ . Such cochain complex on  $\mathcal{M}^G$  has the following form

$$0 \xrightarrow{\text{id}} \mathcal{A}^0(\mathcal{M}^G) \xrightarrow{\partial^0} \mathcal{A}^1(\mathcal{M}^G) \xrightarrow{\partial^1} \mathcal{A}^2(\mathcal{M}^G) \xrightarrow{\partial^2} \mathcal{A}^3(\mathcal{M}^G) \xrightarrow{0} 0.$$

What interests us in this complex is that the DOFs in  $\mathcal{A}^0(\mathcal{M}^G)$  are assigned to the vertices of  $\mathcal{M}^G$ , in  $\mathcal{A}^1(\mathcal{M}^G)$  to the (oriented) edges, in  $\mathcal{A}^2(\mathcal{M}^G)$  to the (oriented) faces and in  $\mathcal{A}^3(\mathcal{M}^G)$  to the (oriented) volumes.

Let now  $G$  be the identity map and  $\mathfrak{X}$  be the complex of the full spline space on  $\Omega$  reported in the third row of the scheme in Figure 5. The control mesh  $\mathcal{M}^G$  in this case is a tensor mesh  $\mathcal{M}$  with vertices of indices  $\{(i, j, k) : i = 1, \dots, n^r; j = 1, \dots, n^s; k = 1, \dots, n^t\}$  called **Greville mesh** [11, Section 3.2.1]. Then, there is a one-to-one correspondence between

- the DOFs in  $\mathbb{S}^{p^r, p^s, p^t}$  and the vertices of  $\mathcal{M}$ ,
- the DOFs in  $\mathbb{S}^{p^r-1, p^s, p^t} \times \mathbb{S}^{p^r, p^s-1, p^t} \times \mathbb{S}^{p^r, p^s, p^t-1}$  and the (oriented) edges in  $\mathcal{M}$ ,
- the DOFs in  $\mathbb{S}^{p^r, p^s-1, p^t-1} \times \mathbb{S}^{p^r-1, p^s, p^t-1} \times \mathbb{S}^{p^r-1, p^s-1, p^t}$  and the (oriented) faces in  $\mathcal{M}$ ,
- the DOFs in  $\mathbb{S}^{p^r-1, p^s-1, p^t}$  and the (oriented) volumes, or elements, in  $\mathcal{M}$ .

A similar matching of DOFs to geometric entities holds when considering the reduced spaces  $V_0, V_1, V_2, V_3$ . This time we take  $G$  as the following  $C^1$  parametrization of the toroidal domain:

$$G(r, s, t) := \sum_{\ell=1}^{n_0} \mathbf{G}_\ell N_\ell^{(0)}(r, s, t) \quad \text{for } (r, s, t) \in \Omega \quad (13)$$

where the  $\mathbf{G}_\ell$  have the following expressions:

$$\mathbf{G}_{1+(k-1)(n^r(n^s-2)+3)} = ((\bar{\rho} + \rho_2) \cos \varphi_k, (\bar{\rho} + \rho_2) \sin \varphi_k, 0)^T$$

$$\mathbf{G}_{2+(k-1)(n^r(n^s-2)+3)} = ((\bar{\rho} - \frac{1}{2}\rho_2) \cos \varphi_k, (\bar{\rho} - \frac{1}{2}\rho_2) \sin \varphi_k, \frac{\sqrt{3}}{2}\rho_2)^T$$

$$\mathbf{G}_{3+(k-1)(n^r(n^s-2)+3)} = ((\bar{\rho} - \frac{1}{2}\rho_2) \cos \varphi_k, (\bar{\rho} - \frac{1}{2}\rho_2) \sin \varphi_k, -\frac{\sqrt{3}}{2}\rho_2)^T$$

$$\mathbf{G}_{3+i+(j-3)n^r+(k-1)(n^r(n^s-2)+3)} = \mathbf{F}_{ijk} \quad \text{for } i = 1, \dots, n^r; j = 3, \dots, n^s; k = 1, \dots, n^t;$$

This time [11, Proposition 4.4] guarantees that the DOFs in the complex of the reduced spline spaces (reported in the fourth row of the scheme in Figure 5) are related to the DOFs in the cochain complex of the control mesh  $\mathcal{R} := \mathcal{M}^G$ , represented in Figure 6.  $\mathcal{R}$  is a polygonal ring composed of  $n^t$  sides connecting at joints which have the shape of a net made of  $n^s - 2$  concentric polygons of  $n^r$  vertices plus three further equidistant vertices lying on a circumference at the center. In particular the DOFs in  $V_0$  are linked to the  $n_0$  vertices of  $\mathcal{R}$  and the DOFs in the spaces we are going to define in the next sections,  $V_1, V_2$  and  $V_3$ , will be related to the oriented edges, faces and volumes in  $\mathcal{R}$ , respectively. Figure 7 shows this geometric interpretation of the DOFs when taking a function  $f \in V_0$  and in  $\mathbb{S}^{p^r, p^s, p^t}$ . As we have observed in Remark 2.1, the DOFs in  $V_0$  are linked to the DOFs in  $\mathbb{S}^{p^r, p^s, p^t}$  via the transpose of  $E^{(0,0,0)}$ .

### 3.3. The gradient of functions in $V_0$ , the operator $\mathcal{E}^1$ and the space $V_1$

Let  $f \in \mathbb{S}^{p^r, p^s, p^t}$ ,  $f = \mathbf{B}^{(0,0,0)} \cdot \mathbf{f}$  for  $\mathbf{f} = (f_1, \dots, f_{n^r n^s n^t})^T$ . In order to simplify the notation, let again  $f_{ijk} = f_{i+(j-1)n^r+(k-1)n^r n^s}$ . The partial derivatives of  $f$  have the following expressions:

$$\frac{\partial}{\partial r} f = \sum_{k=1}^{n^t} \sum_{j=1}^{n^s} \sum_{i=1}^{n^r} (f_{(i+1)jk} - f_{ijk}) B_i^{p^r} B_j^{p^s} B_k^{p^t} \quad (\text{with the convention } "n^r + 1 = 1"),$$

$$\frac{\partial}{\partial s} f = \sum_{k=1}^{n^t} \sum_{j=1}^{n^s-1} \sum_{i=1}^{n^r} (f_{i(j+1)k} - f_{ijk}) B_i^{p^r} B_j^{p^s} B_k^{p^t},$$

$$\frac{\partial}{\partial t} f = \sum_{k=1}^{n^t} \sum_{j=1}^{n^s} \sum_{i=1}^{n^r} (f_{ij(k+1)} - f_{ijk}) B_i^{p^r} B_j^{p^s} B_k^{p^t} \quad (\text{with the convention } "n^t + 1 = 1"),$$

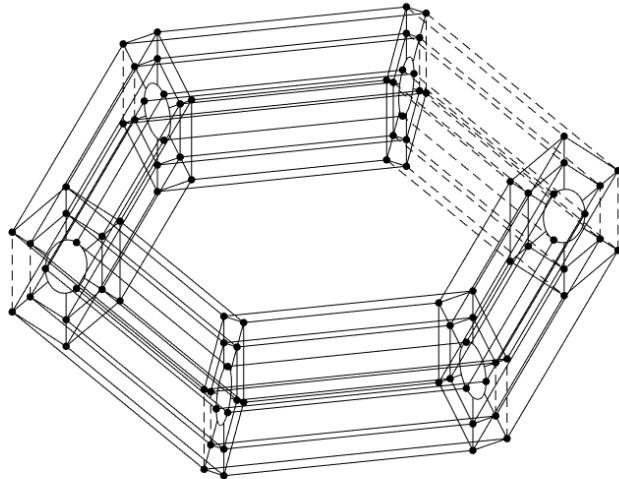


Figure 6: Part of the control mesh  $\mathcal{R}$  associated to the geometry map  $G$  of Equation (13). We show only the first two rounds of control points in the radial direction for the readability of the figure.

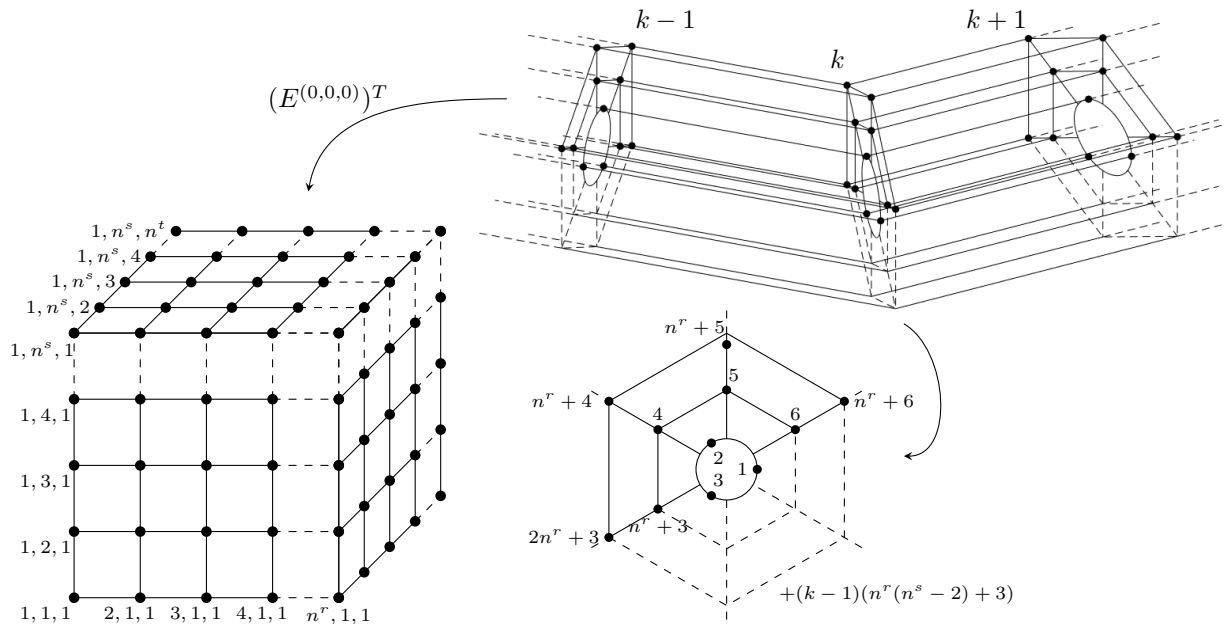


Figure 7: Geometric interpretation of the DOFs of a function in  $\mathbb{S}^{p^r, p^s, p^t}$  (left) and  $V_0$  (right). In the former space, the DOFs are associated to the vertices of a tensor mesh. In the latter they are associated to the vertices of a polygonal ring, partially represented here, in which the joints between two sides are nets of concentric polygons. In the middle figure we show the numbering of the vertices corresponding to the DOFs in  $V_0$  for the  $k$ th joint, with  $k \in \{1, \dots, n^t\}$ . After the first three vertices in the center, we count clockwise the vertices of the concentric polygons from any radial halfline starting at the circumference. When considering a spline in  $V_0$ , one can get its representation in terms of the basis functions of  $\mathbb{S}^{p^r, p^s, p^t}$  by applying the transpose of  $E^{(0,0,0)}$  defined in (11).

where the functions  $D_i^{p^r}, D_j^{p^s}, D_k^{p^t}$ , for any  $i, j, k$ , have been defined in Section 2.1. Let  $\mathbf{B}^{(1,0,0)}, \mathbf{B}^{(0,1,0)}$  and  $\mathbf{B}^{(0,0,1)}$  be the vectorizations of  $\{D_i^{p^r} B_j^{p^s} B_k^{p^t}\}_{i,j,k=1}^{n^r, n^s, n^t}$ ,  $\{B_i^{p^r} D_j^{p^s} B_k^{p^t}\}_{i,j,k=1}^{n^r, n^s-1, n^t}$  and  $\{B_i^{p^r} B_j^{p^s} D_k^{p^t}\}_{i,j,k=1}^{n^r, n^s, n^t}$ , respectively, running the indices on  $i$ , then on  $j$  and then on  $k$ . The gradient operator  $\text{grad} : \mathbb{S}^{p^r, p^s, p^t} \rightarrow \mathbb{S}^{p^r-1, p^s, p^t} \times \mathbb{S}^{p^r, p^s-1, p^t} \times \mathbb{S}^{p^r, p^s, p^t-1}$  has the following matrix representation:

$$\text{grad}f = \begin{pmatrix} \mathbf{B}^{(1,0,0)} \cdot D^{(1,0,0)} \mathbf{f} \\ \mathbf{B}^{(0,1,0)} \cdot D^{(0,1,0)} \mathbf{f} \\ \mathbf{B}^{(0,0,1)} \cdot D^{(0,0,1)} \mathbf{f} \end{pmatrix} \quad \forall f \in \mathbb{S}^{p^r, p^s, p^t},$$

where  $D^{(1,0,0)}, D^{(0,1,0)}$  and  $D^{(0,0,1)}$  are matrices of size  $n^r n^s n^t \times n^r n^s n^t$ ,  $n^r (n^s - 1) n^t \times n^r n^s n^t$  and  $n^r n^s n^t \times n^r n^s n^t$ , respectively, defined as

$$\begin{aligned} D^{(1,0,0)} &= I_{n^t} \otimes I_{n^s} \otimes \mathfrak{D}_{n^r, \mathcal{O}}, \\ D^{(0,1,0)} &= I_{n^t} \otimes \mathfrak{D}_{n^s} \otimes I_{n^r}, \\ D^{(0,0,1)} &= \mathfrak{D}_{n^t, \mathcal{O}} \otimes I_{n^s} \otimes I_{n^r}, \end{aligned} \tag{14}$$

with the use of the following notation: for any  $q \in \mathbb{N}$ ,  $I_q$  is the identity matrix of size  $q$ ,  $\mathfrak{D}_q$  is the matrix of size  $(q - 1) \times q$  whose structure and entries are presented in Equation (5) and  $\mathfrak{D}_{q, \mathcal{O}}$  is the square matrix of size  $q$  whose structure and entries are presented in Equation (6).

We can give a geometric interpretation of the action of the gradient in  $\mathbb{S}^{p^r, p^s, p^t}$ . We have seen that the DOFs in  $\mathbb{S}^{p^r, p^s, p^t}$  and  $\mathbb{S}^{p^r-1, p^s, p^t} \times \mathbb{S}^{p^r, p^s-1, p^t} \times \mathbb{S}^{p^r, p^s, p^t-1}$  can be associated respectively to the vertices and the (oriented) edges of a tensor mesh  $\mathcal{M}$ . In particular the DOFs in  $\text{im}(\text{grad})$  have form

$$\begin{cases} g_{ijk}^1 = f_{(i+1)jk} - f_{ijk} & \text{for } i = 1, \dots, n^r; j = 1, \dots, n^s; k = 1, \dots, n^t; \\ g_{ijk}^2 = f_{i(j+1)k} - f_{ijk} & \text{for } i = 1, \dots, n^r; j = 1, \dots, n^s - 1; k = 1, \dots, n^t; \\ g_{ijk}^3 = f_{ij(k+1)} - f_{ijk} & \text{for } i = 1, \dots, n^r; j = 1, \dots, n^s; k = 1, \dots, n^t; \end{cases} \tag{15}$$

with the conventions “ $n^r + 1 = 1$ ” and “ $n^t + 1 = 1$ ”, for some set of DOFs in  $\mathbb{S}^{p^r, p^s, p^t}$ ,  $\{f_{ijk}\}_{i,j,k=1}^{n^r, n^s, n^t}$ . If this latter are assigned to the vertices of  $\mathcal{M}$ , then the differences in (15) identify particular oriented edges on  $\mathcal{M}$ . For example  $g_{ijk}^1$  is referred to the edge between the vertices  $(i, j, k)$  and  $(i + 1, j, k)$  oriented from the former towards the latter. This interpretation is represented in Figure 8.

Let now  $f \in V_0$ ,  $f = \mathbf{N}^{(0)} \cdot \mathbf{f}$  for  $\mathbf{f} = (f_1, \dots, f_{n_0})^T$ . In order to simplify the notation in what follows, let  $\bar{n}_0 := \frac{n_0}{n^t} = n^r(n^s - 2) + 3$  and  $\bar{n}_1 = 2(\bar{n}_0 - 2)$ . We want the action of the gradient on the DOFs in  $V_0$  to mimic the action we had on the DOFs in  $\mathbb{S}^{p^r, p^s, p^t}$ . This time the collection  $\{f_\ell\}_{\ell=1}^{n_0}$  corresponds to the vertices of the polygonal ring  $\mathcal{R}$  introduced in Section 3.2. The action of the gradient should then associate them to oriented edges in  $\mathcal{R}$ , as shown in Figure 9. The numbers of vertices and edges in a joint of  $\mathcal{R}$  are  $\bar{n}_0$  and  $\bar{n}_1$  respectively. Hence, the total number of edges in  $\mathcal{R}$  is equal to  $n_1 := n^t(\bar{n}_0 + \bar{n}_1) = n^t(3n^r(n^s - 2) + 5)$ , as each vertex in a joint corresponds to an edge of  $\mathcal{R}$  connecting such joint to the next joint. The gradient action on the DOFs of  $V_0$  is therefore encoded by the matrix  $D^{(0)}$  of size  $n_1 \times n_0$ , which, when applied to

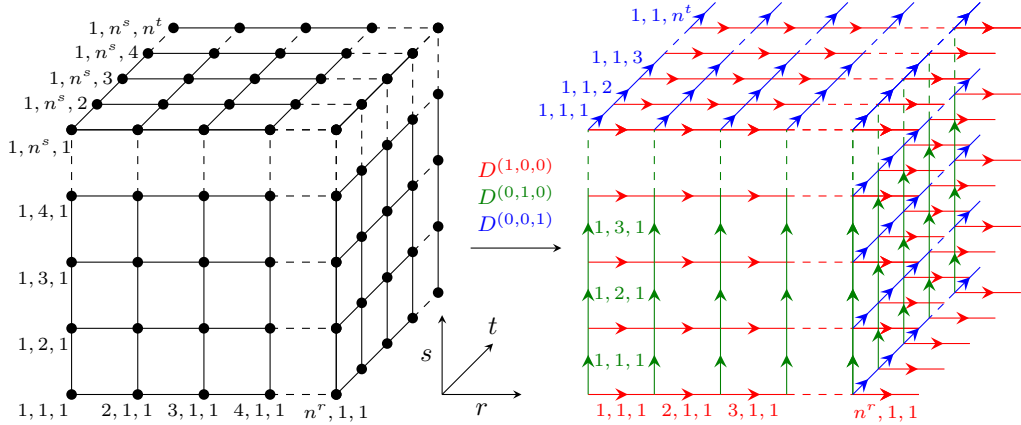


Figure 8: The action of the gradient operator when associating the DOFs in  $\mathbb{S}^{p^r, p^s, p^t}$  to the vertices of a tensor mesh  $\mathcal{M}$ . In the gradient space  $\mathbb{S}^{p^r-1, p^s, p^t} \times \mathbb{S}^{p^r, p^s-1, p^t} \times \mathbb{S}^{p^r, p^s, p^{t-1}}$  the DOFs correspond to oriented edges. In particular in  $\text{im}(\text{grad})$  the first components of the DOFs correspond to the edges in the  $r$  direction, the second components to the edges in the  $s$  direction and the third components to the edges in the  $t$  direction. Because of the periodicity of  $\mathbb{S}^{p^r}$  and  $\mathbb{S}^{p^t}$ , there should be oriented edges connecting the right side with the left side of  $\mathcal{M}$  and the back side with the front side of  $\mathcal{M}$ . These are instead represented in the right figure as arrows going outward of  $\mathcal{M}$ .

$\mathbf{f}$ , provides a vector  $\mathbf{g} = D^{(0)}\mathbf{f}$  with the entries  $\{g_\ell\}_{\ell=1}^{n_1}$  given by

**for**  $k = 1, \dots, n^t$   

$$g_{1+(k-1)(\bar{n}_0+\bar{n}_1)} = f_{2+(k-1)\bar{n}_0} - f_{1+(k-1)\bar{n}_0};$$

$$g_{2+(k-1)(\bar{n}_0+\bar{n}_1)} = f_{3+(k-1)\bar{n}_0} - f_{1+(k-1)\bar{n}_0};$$
**for**  $i = 1, \dots, n^r$   

$$g_{2+i+(k-1)(\bar{n}_0+\bar{n}_1)} = f_{3+i+(k-1)\bar{n}_0} - \sum_{\ell=1}^3 \bar{E}_{\ell,(i,2)} f_{\ell+(k-1)\bar{n}_0};$$
**for**  $j = 3, \dots, n^s - 1$   
**for**  $i = 1, \dots, n^r$   

$$g_{2+i+(2j-5)n^r+(k-1)(\bar{n}_0+\bar{n}_1)} = f_{4+i+(j-3)n^r+(k-1)\bar{n}_0} - f_{3+i+(j-3)n^r+(k-1)\bar{n}_0};$$

$$g_{2+i+(2j-4)n^r+(k-1)(\bar{n}_0+\bar{n}_1)} = f_{3+i+(j-2)n^r+(k-1)\bar{n}_0} - f_{3+i+(j-3)n^r+(k-1)\bar{n}_0};$$
**for**  $i = 1, \dots, n^r$   

$$g_{2+i+(2n^s-5)n^r+(k-1)(\bar{n}_0+\bar{n}_1)} = f_{4+i+(n^s-3)n^r+(k-1)\bar{n}_0} - f_{3+i+(n^s-3)n^r+(k-1)\bar{n}_0};$$
**for**  $i = 1, \dots, \bar{n}_0$   

$$g_{i+k\bar{n}_1+(k-1)\bar{n}_0} = f_{i+k\bar{n}_0} - f_{i+(k-1)\bar{n}_0}$$
 (with the convention “ $n^t\bar{n}_0 + i = i'$ ”). (16)

All of such entries are differences of two DOFs in  $V_0$ , corresponding to the endpoints of an edge in  $\mathcal{R}$ , except those whose geometric interpretation forms the first round of radial edges in a joint of  $\mathcal{R}$  from the central circumference, namely  $g_{2+i+(k-1)(\bar{n}_0+\bar{n}_1)}$  for  $i = 1, \dots, n^r$ , for which a suitable combination of the three vertices  $f_{\ell+(k-1)\bar{n}_0}$  for  $\ell = 1, 2, 3$  and  $k \in \{1, \dots, n^t\}$  is invoked. The coefficients  $\bar{E}_{\ell,(i,2)}$  for  $i = 1, \dots, n^r$  are taken from the block  $\bar{E}$  of matrix  $E^{(0)}$  in Equation (12).

Let us indicate as  $\mathcal{E}^1 : \mathbb{S}^{p^r-1, p^s, p^t} \times \mathbb{S}^{p^r, p^s-1, p^t} \times \mathbb{S}^{p^r, p^s, p^t-1} \rightarrow V_1$  the extraction operator defining the space  $V_1$  containing the gradients of the functions in  $V_0$ . In order to simplify the coming matrix representation of  $\mathcal{E}^1$ , we introduce the following notation.

Given two matrices  $A$  and  $B$  with the same number of columns and, possibly, with a different number of rows, let  $[A; B]$  be the matrix obtained by stacking the rows of  $A$  on top of those of  $B$ .

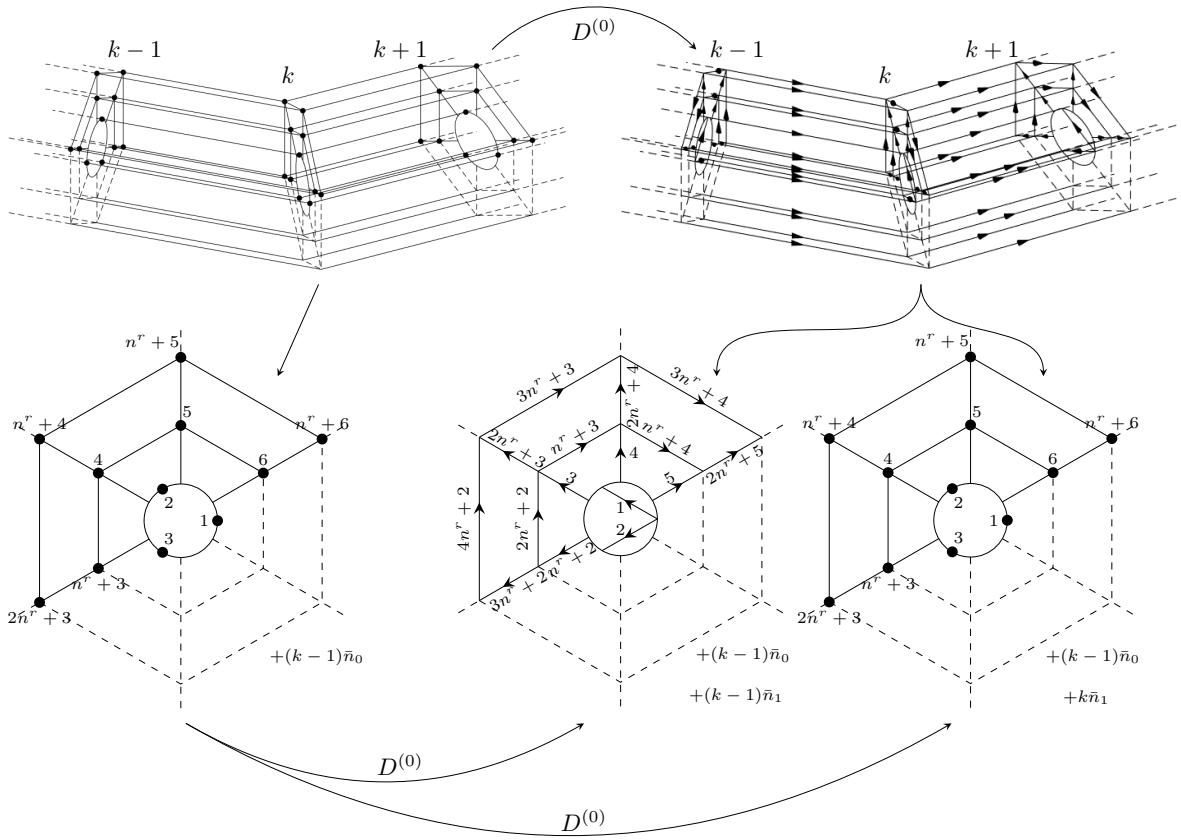


Figure 9: The action of the gradient operator when associating the DOFs in  $V_0$  to the vertices of the polygonal ring  $\mathcal{R}$ . In the gradient space the DOFs correspond to the oriented edges. On the top of the figure we see part of  $\mathcal{R}$ . On the bottom we see the numbering of the vertices (left) and of the edges (right) when considering the  $k$ th joint in  $\mathcal{R}$ , for  $k \in \{1, \dots, n^t\}$ . Note that the edges running around the hole of  $\mathcal{R}$  are represented as dots in the right-most figure when looking at a joint.  $D^{(0)}$  is a matrix mapping the vertices in  $\mathcal{R}$  to the oriented edges in  $\mathcal{R}$  and encodes the geometric interpretation of the gradient action on the DOFs.

With this notation at hand, let now  $E^{(1,0,0)}$ ,  $E^{(0,1,0)}$  and  $E^{(0,0,1)}$  be the following matrices:

$$\begin{aligned} E^{(1,0,0)} &= I_{n^t} \otimes [E^{(1,0)}; O^{(1,0,0)}], \\ E^{(0,1,0)} &= I_{n^t} \otimes [E^{(0,1)}; O^{(0,1,0)}], \\ E^{(0,0,1)} &= I_{n^t} \otimes [O^{(0,0,1)}; E^{(0)}], \end{aligned} \quad (17)$$

where  $O^{(1,0,0)}$ ,  $O^{(0,1,0)}$  and  $O^{(0,0,1)}$  are zero matrices of size  $\bar{n}_0 \times n^r n^s$ ,  $\bar{n}_0 \times n^r(n^s - 1)$  and  $\bar{n}_1 \times n^r n^s$ , respectively,  $E^{(0)}$  is the matrix of Equation (12) and  $E^{(1,0)}$ ,  $E^{(0,1)}$  are two matrices, introduced in [35], of size  $\bar{n}_1 \times n^r n^s$  and  $\bar{n}_1 \times n^r(n^s - 1)$ , defined by their actions as

$$\begin{aligned} E^{(1,0)} \mathbf{x} &=: \mathbf{y} \text{ whose components are} \\ \text{for } \ell &= 1, 2 \\ &\quad \left| \begin{array}{l} y_\ell = \sum_{i=1}^{n^r} (\bar{E}_{\ell+1,(i+1,2)} - \bar{E}_{\ell+1,(i,2)}) x_{i+n^r}; \\ \text{for } j = 3, \dots, n^s \\ \quad \text{for } i = 1, \dots, n^r \\ \quad \left| \begin{array}{l} y_{2+i+(2j-6)n^r} = 0; \\ y_{2+i+(2j-5)n^r} = x_{i+(j-1)n^r}; \end{array} \right. \end{array} \right. \\ &\quad \text{(with the convention "} n^r + 1 = 1 \text{"),} \\ E^{(0,1)} \mathbf{x} &=: \mathbf{y} \text{ whose components are} \\ \text{for } \ell &= 1, 2 \\ &\quad \left| \begin{array}{l} y_\ell = \sum_{i=1}^{n^r} (\bar{E}_{\ell+1,(i,2)} - \bar{E}_{\ell+1,(i,1)}) x_i; \\ \text{for } j = 2, \dots, n^s - 1 \\ \quad \text{for } i = 1, \dots, n^r \\ \quad \left| \begin{array}{l} y_{2+i+(2j-4)n^r} = x_{i+(j-1)n^r}; \\ y_{2+i+(2j-3)n^r} = 0; \end{array} \right. \end{array} \right. \end{aligned} \quad (18)$$

where  $\bar{E}_{\ell+1,(i,j)}$  are entries of the block  $\bar{E}$  in matrix  $E^{(0)}$  of Equation (12).  $E^{(1,0,0)}$ ,  $E^{(0,1,0)}$  and  $E^{(0,0,1)}$  have sizes  $n_1 \times n^r n^s n^t$ ,  $n_1 \times n^r(n^s - 1)n^t$  and  $n_1 \times n^r n^s n^t$  respectively. These matrices will provide the relation between the DOFs in  $V_1$  and  $\mathbb{S}^{p^r-1,p^s,p^t} \times \mathbb{S}^{p^r,p^s-1,p^t} \times \mathbb{S}^{p^r,p^s,p^t-1}$ , accordingly to Remark 2.1. Namely, given a set of DOFs in  $V_1$ ,  $\mathbf{g} = \{g_\ell\}_{\ell=1}^{n_1}$ , we will have that

$$\begin{aligned} \mathbf{g}^1 &= (E^{(1,0,0)})^T \mathbf{g}, \\ \mathbf{g}^2 &= (E^{(0,1,0)})^T \mathbf{g}, \\ \mathbf{g}^3 &= (E^{(0,0,1)})^T \mathbf{g}, \end{aligned} \quad (19)$$

where  $\mathbf{g}^1, \mathbf{g}^2, \mathbf{g}^3$  are the vectorizations of the DOFs in the first, second and third components of an element  $g$  in  $\mathbb{S}^{p^r-1,p^s,p^t} \times \mathbb{S}^{p^r,p^s-1,p^t} \times \mathbb{S}^{p^r,p^s,p^t-1}$ , i.e.,

$$g = \begin{pmatrix} g^1 \\ g^2 \\ g^3 \end{pmatrix} = \begin{pmatrix} \mathbf{B}^{(1,0,0)} \cdot \mathbf{g}^1 \\ \mathbf{B}^{(0,1,0)} \cdot \mathbf{g}^2 \\ \mathbf{B}^{(0,0,1)} \cdot \mathbf{g}^3 \end{pmatrix} \in \mathbb{S}^{p^r-1,p^s,p^t} \times \mathbb{S}^{p^r,p^s-1,p^t} \times \mathbb{S}^{p^r,p^s,p^t-1}.$$

The geometric interpretation of this link between the DOFs in  $V_1$  and in  $\mathbb{S}^{p^r-1,p^s,p^t} \times \mathbb{S}^{p^r,p^s-1,p^t} \times \mathbb{S}^{p^r,p^s,p^t-1}$  is pictured in Figure 10.

**Proposition 3.1.** *Let us indicate with*

- $\{f_{ijk}\}_{i,j,k=1}^{n^r,n^s,n^t}$  a general set of DOFs in  $\mathbb{S}^{p^r,p^s,p^t}$ ,
- $\{g_{ijk}^1\}_{i,j,k=1}^{n^r,n^s,n^t}, \{g_{ijk}^2\}_{i,j,k=1}^{n^r,n^s-1,n^t}, \{g_{ijk}^3\}_{i,j,k=1}^{n^r,n^s,n^t}$  a general set of DOFs in  $im(\text{grad}) \subseteq \mathbb{S}^{p^r-1,p^s,p^t} \times \mathbb{S}^{p^r,p^s-1,p^t} \times \mathbb{S}^{p^r,p^s,p^t-1}$ ,
- $\{f_\ell\}_{\ell=1}^{n_0}$  a general set of DOFs in  $V_0$ ,

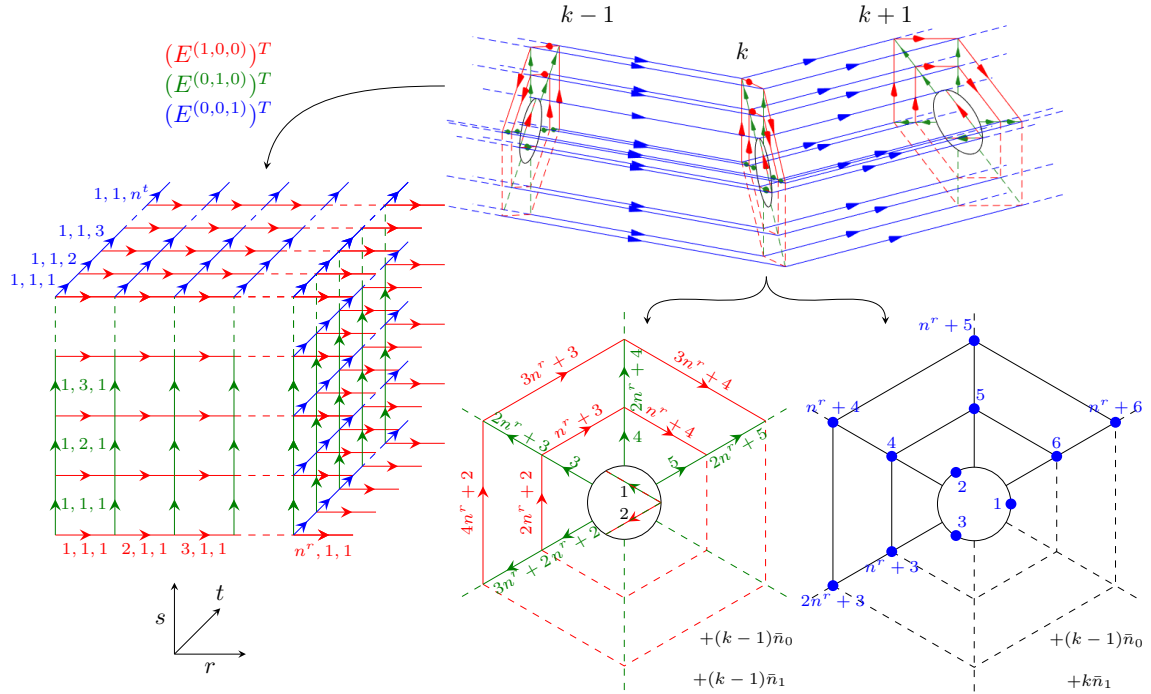


Figure 10: Geometric interpretation of the DOFs in the gradient spaces  $\mathbb{S}^{p^r-1, p^s, p^t} \times \mathbb{S}^{p^r, p^s-1, p^t} \times \mathbb{S}^{p^r, p^s, p^t-1}$  (left) and  $V_1$  (right). In the former space, the DOFs are associated to the oriented edges of a tensor mesh  $\mathcal{M}$ . In the latter they are associated to the oriented edges of a polygonal ring  $\mathcal{R}$ , defined in Section 3.2 and partially represented here. In the middle figure we show the numbering of the edges corresponding to the DOFs in  $V_1$  from the point of view of the  $k$ th joint, with  $k \in \{1, \dots, n^t\}$ . The edges moving from the  $k$ th joint to the  $(k+1)$ th joint are represented as dots in the right-most figure. When considering a gradient function in  $V_1$ , one can get its representation in terms of the basis functions in  $\mathbb{S}^{p^r-1, p^s, p^t} \times \mathbb{S}^{p^r, p^s-1, p^t} \times \mathbb{S}^{p^r, p^s, p^t-1}$  by applying the transpose of the matrices  $E^{(1,0,0)}$ ,  $E^{(0,1,0)}$  and  $E^{(0,0,1)}$  defined in (17). More precisely,  $(E^{(1,0,0)})^T$ ,  $(E^{(0,1,0)})^T$  and  $(E^{(0,0,1)})^T$  link the DOFs corresponding to poloidal, radial and toroidal edges in  $\mathcal{R}$ , respectively, with the DOFs relative to the edges in the  $r$ ,  $s$  and  $t$  directions, respectively, of the tensor mesh  $\mathcal{M}$ . The first two edges in a joint of  $\mathcal{R}$  are neither radial nor poloidal. They are linked to edges of  $\mathcal{M}$  both in the  $r$  and in the  $s$  directions.

- $\{g_\ell\}_{\ell=1}^{n_1}$  the collection of numbers such that Equation (19) holds true for any given choice of the DOFs  $\{g_{ijk}^1\}_{i,j,k=1}^{n^r, n^s, n^t}, \{g_{ijk}^2\}_{i,j,k=1}^{n^r, n^s-1, n^t}, \{g_{ijk}^3\}_{i,j,k=1}^{n^r, n^s, n^t}$ .

Then the following diagrams commute:

$$\begin{array}{ccc}
\begin{array}{c}
\{f_{ijk}\}_{i,j,k=1}^{n^r, n^s, n^t} \xrightarrow{D^{(1,0,0)}} \{g_{ijk}^1\}_{i,j,k=1}^{n^r, n^s, n^t} \\
\uparrow (E^{(0,0,0)})^T \quad \uparrow (E^{(1,0,0)})^T \\
\{f_\ell\}_{\ell=1}^{n_0} \xrightarrow[D^{(0)}]{} \{g_\ell\}_{\ell=1}^{n_1}
\end{array}
&
\begin{array}{c}
\{f_{ijk}\}_{i,j,k=1}^{n^r, n^s, n^t} \xrightarrow{D^{(0,1,0)}} \{g_{ijk}^2\}_{i,j,k=1}^{n^r, n^s-1, n^t} \\
\uparrow (E^{(0)})^T \quad \uparrow (E^{(0,1,0)})^T \\
\{f_\ell\}_{\ell=1}^{n_0} \xrightarrow[D^{(0)}]{} \{g_\ell\}_{\ell=1}^{n_1}
\end{array}
\\
(a) \qquad \qquad \qquad (b) \\
\begin{array}{c}
\{f_{ijk}\}_{i,j,k=1}^{n^r, n^s, n^t} \xrightarrow{D^{(0,0,1)}} \{g_{ijk}^3\}_{i,j,k=1}^{n^r, n^s, n^t} \\
\uparrow (E^{(0)})^T \quad \uparrow (E^{(0,0,1)})^T \\
\{f_\ell\}_{\ell=1}^{n_0} \xrightarrow[D^{(0)}]{} \{g_\ell\}_{\ell=1}^{n_1}
\end{array}
\\
(c)
\end{array}$$

*Proof.* The proof of commutation is similar for all the three diagrams. In order to simplify notation in what follows, we define

$$\begin{aligned}
\bar{E}_{\ell,(\Delta i,j)} &:= \bar{E}_{\ell,(i+1,j)} - \bar{E}_{\ell,(i,j)} \quad (\text{with the convention } "n^r + 1 = 1"), \\
\bar{E}_{\ell,(i,2-1)} &:= \bar{E}_{\ell,(i,2)} - \bar{E}_{\ell,(i,1)},
\end{aligned} \tag{20}$$

where  $\bar{E}_{\ell,(i,j)}$ , for  $\ell = 1, 2, 3$ ,  $i = 1, \dots, n^r$  and  $j = 1, 2$ , are the elements of the block  $\bar{E}$  of matrix  $E^{(0)}$  reported in Equation (12). Let us start with diagram (a). We go around it in a sequence of identities, making a loop from  $g_{ijk}^1$  back to itself. We treat separately the cases  $j \leq 2$  and  $j \geq 3$ . By using the fact that matrix  $E^{(0)}$  is DTA-compatible, so that in particular its columns sum to one, for  $j \leq 2$  we have

$$\begin{aligned}
g_{ijk}^1 &\stackrel{D^{(1,0,0)}}{=} f_{(i+1)jk} - f_{ijk} \quad (\text{with the convention } "n^r + 1 = 1") \\
&\stackrel{(E^{(0)})^T}{=} \sum_{\ell=1}^3 \bar{E}_{\ell,(i+1,j)} f_{\ell+(k-1)\bar{n}_0} - \sum_{\ell=1}^3 \bar{E}_{\ell,(i,j)} f_{\ell+(k-1)\bar{n}_0} \\
&= \sum_{\ell=1}^3 \bar{E}_{\ell,(\Delta i,j)} f_{\ell+(k-1)\bar{n}_0} + f_{1+(k-1)\bar{n}_0} - f_{1+(k-1)\bar{n}_0} \\
&\stackrel{\text{DTA}}{=} \sum_{\ell=1}^3 \bar{E}_{\ell,(\Delta i,j)} f_{\ell+(k-1)\bar{n}_0} + \sum_{\ell=1}^3 \bar{E}_{\ell,(i+1,j)} f_{1+(k-1)\bar{n}_0} - \sum_{\ell=1}^3 \bar{E}_{\ell,(i,j)} f_{1+(k-1)\bar{n}_0} \\
&= \sum_{\ell=1}^2 \bar{E}_{\ell+1,(\Delta i,j)} (f_{(\ell+1)+(k-1)\bar{n}_0} - f_{1+(k-1)\bar{n}_0}) \\
&\stackrel{D^{(0)}}{=} \sum_{\ell=1}^2 \bar{E}_{\ell+1,(\Delta i,j)} g_{\ell+(k-1)(\bar{n}_0+\bar{n}_1)} \stackrel{(E^{(1,0,0)})^T}{=} g_{ijk}^1,
\end{aligned}$$

where in the last equality for  $j = 1$ , we have used that  $\bar{E}_{\ell,(\Delta i,1)} = 0$  for all  $\ell$  and  $i$ . For  $j \geq 3$  the proof is

simpler:

$$\begin{aligned}
g_{ijk}^1 &\stackrel{D^{(1,0,0)}}{=} f_{(i+1)jk} - f_{ijk} \quad (\text{with the convention } "n^r + 1 = 1") \\
&\stackrel{(E^{(0)})^T}{=} f_{4+i+(j-3)n^r+(k-1)\bar{n}_0} - f_{3+i+(j-3)n^r+(k-1)\bar{n}_0} \\
&\stackrel{D^{(0)}}{=} g_{2+i+(2j-5)n^r+(k-1)(\bar{n}_0+\bar{n}_1)} \stackrel{(E^{(1,0,0)})^T}{=} g_{ijk}^1.
\end{aligned}$$

This completes the proof of commutation in diagram (a). Let us move to diagram (b). This time we treat the cases  $j = 1, j = 2$  and  $j \geq 3$  separately. For  $j = 1$  we have

$$\begin{aligned}
g_{i1k}^2 &\stackrel{D^{(0,1,0)}}{=} f_{i2k} - f_{i1k} \\
&\stackrel{(E^{(0)})^T}{=} \sum_{\ell=1}^3 \bar{E}_{\ell,(i,2)} f_{\ell+(k-1)\bar{n}_0} - \sum_{\ell=1}^3 \bar{E}_{\ell,(i,1)} f_{\ell+(k-1)\bar{n}_0} \\
&= \sum_{\ell=1}^3 \bar{E}_{\ell,(i,2-1)} f_{\ell+(k-1)\bar{n}_0} + f_{1+(k-1)\bar{n}_0} - f_{1+(k-1)\bar{n}_0} \\
&\stackrel{\text{DTA}}{=} \sum_{\ell=1}^3 \bar{E}_{\ell,(i,2-1)} f_{\ell+(k-1)\bar{n}_0} + \sum_{\ell=1}^3 \bar{E}_{\ell,(i,2)} f_{1+(k-1)\bar{n}_0} - \sum_{\ell=1}^3 \bar{E}_{\ell,(i,1)} f_{1+(k-1)\bar{n}_0} \\
&= \sum_{\ell=1}^2 \bar{E}_{\ell+1,(i,2-1)} (f_{(\ell+1)+(k-1)\bar{n}_0} - f_{1+(k-1)\bar{n}_0}) \\
&\stackrel{D^{(0)}}{=} \sum_{\ell=1}^2 \bar{E}_{\ell+1,(i,2-1)} g_{\ell+(k-1)(\bar{n}_0+\bar{n}_1)} \stackrel{(E^{(0,1,0)})^T}{=} g_{i1k}^2.
\end{aligned}$$

For  $j = 2$  and  $j \geq 3$  the proof is simpler. When  $j = 2$  it holds

$$\begin{aligned}
g_{i2k}^2 &\stackrel{D^{(0,1,0)}}{=} f_{i3k} - f_{i2k} \\
&\stackrel{(E^{(0)})^T}{=} f_{i+3+(k-1)\bar{n}_0} - \sum_{\ell=1}^3 \bar{E}_{\ell,(i,2)} f_{\ell+(k-1)\bar{n}_0} \\
&\stackrel{D^{(0)}}{=} g_{i+2+(k-1)(\bar{n}_0+\bar{n}_1)} \stackrel{(E^{(0,1,0)})^T}{=} g_{i2k}^2
\end{aligned}$$

and for  $j \geq 3$  we have

$$\begin{aligned}
g_{ijk}^2 &\stackrel{D^{(0,1,0)}}{=} f_{i(j+1)k} - f_{ijk} \\
&\stackrel{(E^{(0)})^T}{=} f_{i+3+(j-2)n^r+(k-1)\bar{n}_0} - f_{i+3+(j-3)n^r+(k-1)\bar{n}_0} \\
&\stackrel{D^{(0)}}{=} g_{i+2+(2j-4)n^r+(k-1)(\bar{n}_0+\bar{n}_1)} \stackrel{(E^{(0,1,0)})^T}{=} g_{ijk}^2.
\end{aligned}$$

This completes the proof of commutation for diagram (b). Finally, for diagram (c) we consider the cases  $j \leq 2$  and  $j \geq 3$ . In the first, we have

$$\begin{aligned}
g_{ijk}^3 &\stackrel{D^{(0,0,1)}}{=} f_{ij(k+1)} - f_{ijk} \quad (\text{with the convention } "n^t + 1 = 1") \\
&\stackrel{(E^{(0)})^T}{=} \sum_{\ell=1}^3 \bar{E}_{\ell,(i,j)} (f_{\ell+k\bar{n}_0} - f_{\ell+(k-1)\bar{n}_0}) \quad (\text{with the convention } "n^t \bar{n}_0 + \ell = \ell") \\
&\stackrel{D^{(0)}}{=} \sum_{\ell=1}^3 \bar{E}_{\ell,(i,j)} g_{\ell+(k-1)\bar{n}_0+k\bar{n}_1} \stackrel{(E^{(0,0,1)})^T}{=} g_{ijk}^3.
\end{aligned}$$

In the second, it holds

$$\begin{aligned}
g_{ijk}^3 &\stackrel{D^{(0,0,1)}}{=} f_{ij(k+1)} - f_{ijk} \quad ("n^t + 1 = 1") \\
&\stackrel{(E^{(0)})^T}{=} f_{i+3+(j-3)n^r+k\bar{n}_0} - f_{i+3+(j-3)n^r+(k-1)\bar{n}_0} \quad (\text{with the convention } "n^t\bar{n}_0 + m = m") \\
&\stackrel{D^{(0)}}{=} g_{i+3+(j-3)n^r+(k-1)\bar{n}_0+k\bar{n}_1} \stackrel{(E^{(0,0,1)})^T}{=} g_{ijk}^3.
\end{aligned}$$

□

We can finally define  $V_1$  and the extraction operator  $\mathcal{E}^1$ . First, let us introduce the following collections of  $n_1$  functions,

$$\begin{aligned}
\mathbf{N}^{(1,0,0)} &:= E^{(1,0,0)} \mathbf{B}^{(1,0,0)}, \\
\mathbf{N}^{(0,1,0)} &:= E^{(0,1,0)} \mathbf{B}^{(0,1,0)}, \\
\mathbf{N}^{(0,0,1)} &:= E^{(0,0,1)} \mathbf{B}^{(0,0,1)}.
\end{aligned} \tag{21}$$

We highlight that  $\mathbf{N}^{(1,0,0)}$ ,  $\mathbf{N}^{(0,1,0)}$  and  $\mathbf{N}^{(0,0,1)}$  contain zero functions. However, there exist no index  $\ell$  in  $\{1, \dots, n_1\}$  for which  $N_\ell^{(1,0,0)}$ ,  $N_\ell^{(0,1,0)}$  and  $N_\ell^{(0,0,1)}$  are all zero functions. This can be easily seen from the structure of the matrices  $E^{(1,0,0)}$ ,  $E^{(0,1,0)}$ ,  $E^{(0,0,1)}$ , reported in Equation (17), and the entries of the blocks  $E^{(1,0)}$ ,  $E^{(0,1)}$  and  $E^{(0)}$ , shown in Equations (18) and (12).

**Proposition 3.2.** *The non-zero functions in  $\mathbf{N}^{(1,0,0)}$ ,  $\mathbf{N}^{(0,1,0)}$  and  $\mathbf{N}^{(0,0,1)}$ , defined in Equation (21), are linearly independent.*

*Proof.* The functions in  $\mathbf{B}^{(1,0,0)}$ ,  $\mathbf{B}^{(0,1,0)}$  and  $\mathbf{B}^{(0,0,1)}$  are linearly independent. Furthermore, one can show, see [35], that the non-zero rows in  $E^{(0)}$ ,  $E^{(1,0)}$  and  $E^{(0,1)}$  are linearly independent, which implies that the matrices  $E^{(1,0,0)}$ ,  $E^{(0,1,0)}$  and  $E^{(0,0,1)}$  have linearly independent non-zero rows as well, because of Equation (17). By Equation (21), the non-zero functions in  $\mathbf{N}^{(1,0,0)}$ ,  $\mathbf{N}^{(0,1,0)}$  and  $\mathbf{N}^{(0,0,1)}$  are linearly independent. □

We define the space  $V_1$  as the span of the following linearly independent vector functions

$$N_\ell^{(1)} := \begin{pmatrix} N_\ell^{(1,0,0)} \\ N_\ell^{(0,1,0)} \\ N_\ell^{(0,0,1)} \end{pmatrix} \quad \text{for } \ell = 1, \dots, n_1. \tag{22}$$

The extraction operator  $\mathcal{E}^1 : \mathbb{S}^{p^r-1, p^s, p^t} \times \mathbb{S}^{p^r, p^s-1, p^t} \times \mathbb{S}^{p^r, p^s, p^t-1} \rightarrow V_1$  constitutes the collection  $\mathbf{N}^{(1)}$  of the functions reported in Equation (22) from the three sets of B-spline derivatives  $\mathbf{B}^{(1,0,0)}$ ,  $\mathbf{B}^{(0,1,0)}$  and  $\mathbf{B}^{(0,0,1)}$ . With the definition of  $V_1$  at hand and thanks to Remark 2.1, we can rewrite Proposition 3.1 as follows.

**Corollary 3.3.** *The diagram*

$$\begin{array}{ccccc}
\mathbb{S}^{p^r, p^s, p^t} & \xrightarrow{\text{grad}} & \mathbb{S}^{p^r-1, p^s, p^t} \times \mathbb{S}^{p^r, p^s-1, p^t} \times \mathbb{S}^{p^r, p^s, p^t-1} \\
\mathcal{E}^0 \downarrow & \searrow & \downarrow \mathcal{E}^1 \\
V_0 & \xrightarrow{\text{grad}} & V_1
\end{array}$$

commutes and the pushforward of the functions in  $V_1$ , namely  $\mathcal{F}^1(N_\ell^{(1)})$  for  $\ell = 1, \dots, n_1$ , with the operator  $\mathcal{F}^1$  defined as in (8), are  $C^0$  on  $\Omega^{pol}$ .

*Proof.* The commutation is drawn from Proposition 3.1 and Remark 2.1. For what concerns the smoothness of the pushforwarded functions, the  $C^0$ -continuity is implied by their local exactness at the polar curve.  $\square$

We conclude the section clearly stating the representation of the gradient of a function in  $V_0$  in the basis of  $V_1$ . Given  $f \in V_0$ ,  $f = \mathbf{N}^{(0)} \cdot \mathbf{f}$ , we have that

$$\text{grad } f = \mathbf{N}^{(1)} \cdot D^{(0)} \mathbf{f} = \begin{pmatrix} \mathbf{N}^{(1,0,0)} \cdot D^{(0)} \mathbf{f} \\ \mathbf{N}^{(0,1,0)} \cdot D^{(0)} \mathbf{f} \\ \mathbf{N}^{(0,0,1)} \cdot D^{(0)} \mathbf{f} \end{pmatrix} \in V_1.$$

### 3.4. The curl of functions in $V_1$ , the operator $\mathcal{E}^2$ and the space $V_2$

Let  $g \in \mathbb{S}^{p^r-1, p^s, p^t} \times \mathbb{S}^{p^r, p^s-1, p^t} \times \mathbb{S}^{p^r, p^s, p^t-1}$ ,

$$g = \begin{pmatrix} g^1 \\ g^2 \\ g^3 \end{pmatrix} = \begin{pmatrix} \mathbf{B}^{(1,0,0)} \cdot \mathbf{g}^1 \\ \mathbf{B}^{(0,1,0)} \cdot \mathbf{g}^2 \\ \mathbf{B}^{(0,0,1)} \cdot \mathbf{g}^3 \end{pmatrix}$$

with  $\mathbf{g}^1, \mathbf{g}^2, \mathbf{g}^3$  the vectorizations of the coefficients  $\{g_{ijk}^1\}_{i,j,k=1}^{n^r, n^s, n^t}, \{g_{ijk}^2\}_{i,j,k=1}^{n^r, n^s-1, n^t}, \{g_{ijk}^3\}_{i,j,k=1}^{n^r, n^s, n^t}$  obtained by running the indices first on  $i$ , then on  $j$  and then on  $k$ . The curl of  $g$  has the following expression:

$$\text{curl } g = \begin{pmatrix} \sum_{k=1}^{n^t} \sum_{j=1}^{n^s-1} \sum_{i=1}^{n^r} (g_{i(j+1)k}^3 - g_{ijk}^3 + g_{ijk}^2 - g_{ij(k+1)}^2) B_i^{p^r} D_j^{p^s} D_k^{p^t} \\ \sum_{k=1}^{n^t} \sum_{j=1}^{n^s} \sum_{i=1}^{n^r} (g_{ij(k+1)}^1 - g_{ijk}^1 + g_{ijk}^3 - g_{(i+1)jk}^3) D_i^{p^r} B_j^{p^s} D_k^{p^t} \\ \sum_{k=1}^{n^t} \sum_{j=1}^{n^s-1} \sum_{i=1}^{n^r} (g_{(i+1)jk}^2 - g_{ijk}^2 + g_{ijk}^1 - g_{i(j+1)k}^1) D_i^{p^r} D_j^{p^s} B_k^{p^t} \end{pmatrix},$$

where the functions  $D_i^{p^r}, D_j^{p^s}, D_k^{p^t}$ , for any  $i, j, k$ , have been defined in Section 2.1. Let  $\mathbf{B}^{(0,1,1)}, \mathbf{B}^{(1,0,1)}$  and  $\mathbf{B}^{(1,1,0)}$  be the vectorizations of  $\{B_i^{p^r} D_j^{p^s} D_k^{p^t}\}_{i,j,k=1}^{n^r, n^s-1, n^t}, \{D_i^{p^r} B_j^{p^s} D_k^{p^t}\}_{i,j,k=1}^{n^r, n^s, n^t}$  and  $\{D_i^{p^r} D_j^{p^s} B_k^{p^t}\}_{i,j,k=1}^{n^r, n^s-1, n^t}$ , respectively, running the indices on  $i$ , then on  $j$  and then on  $k$ . The curl operator  $\text{curl} : \mathbb{S}^{p^r-1, p^s, p^t} \times \mathbb{S}^{p^r, p^s-1, p^t} \times \mathbb{S}^{p^r, p^s, p^t-1} \rightarrow \mathbb{S}^{p^r, p^s-1, p^t-1} \times \mathbb{S}^{p^r-1, p^s, p^t-1} \times \mathbb{S}^{p^r-1, p^s-1, p^t}$  has the following matrix representation:

$$\text{curl } g = \begin{pmatrix} \mathbf{B}^{(0,1,1)} \cdot [-D^{(0,0,1)} \mathbf{g}^2 + D^{(0,1,0)} \mathbf{g}^3] \\ \mathbf{B}^{(1,0,1)} \cdot [D^{(0,0,1)} \mathbf{g}^1 - D^{(1,0,0)} \mathbf{g}^3] \\ \mathbf{B}^{(1,1,0)} \cdot [-D^{(0,1,0)} \mathbf{g}^1 + D^{(1,0,0)} \mathbf{g}^2] \end{pmatrix} \quad \forall g \in \mathbb{S}^{p^r-1, p^s, p^t} \times \mathbb{S}^{p^r, p^s-1, p^t} \times \mathbb{S}^{p^r, p^s, p^t-1},$$

where the matrices  $D^{(1,0,0)}, D^{(0,1,0)}$  and  $D^{(0,0,1)}$  have been defined in Equation (14). Hence, the DOFs in  $\text{im}(\text{curl})$  have form

$$\begin{cases} h_{ijk}^1 := g_{i(j+1)k}^3 - g_{ijk}^3 + g_{ijk}^2 - g_{ij(k+1)}^2 & \text{for } i = 1, \dots, n^r; j = 1, \dots, n^s-1; k = 1, \dots, n^t; \\ h_{ijk}^2 := g_{ij(k+1)}^1 - g_{ijk}^1 + g_{ijk}^3 - g_{(i+1)jk}^3 & \text{for } i = 1, \dots, n^r; j = 1, \dots, n^s; k = 1, \dots, n^t; \\ h_{ijk}^3 := g_{(i+1)jk}^2 - g_{ijk}^2 + g_{ijk}^1 - g_{i(j+1)k}^1 & \text{for } i = 1, \dots, n^r; j = 1, \dots, n^s-1; k = 1, \dots, n^t; \end{cases}$$

with the conventions “ $n^r + 1 = 1$ ” and “ $n^t + 1 = 1$ ”, for some set of DOFs  $\{g_{ijk}^1\}_{i,j,k=1}^{n^r, n^s, n^t}, \{g_{ijk}^2\}_{i,j,k=1}^{n^r, n^s-1, n^t}, \{g_{ijk}^3\}_{i,j,k=1}^{n^r, n^s, n^t}$  in  $\mathbb{S}^{p^r-1, p^s, p^t} \times \mathbb{S}^{p^r, p^s-1, p^t} \times \mathbb{S}^{p^r, p^s, p^t-1}$ . We have seen the geometric interpretations of  $g_{ijk}^1, g_{ijk}^2$

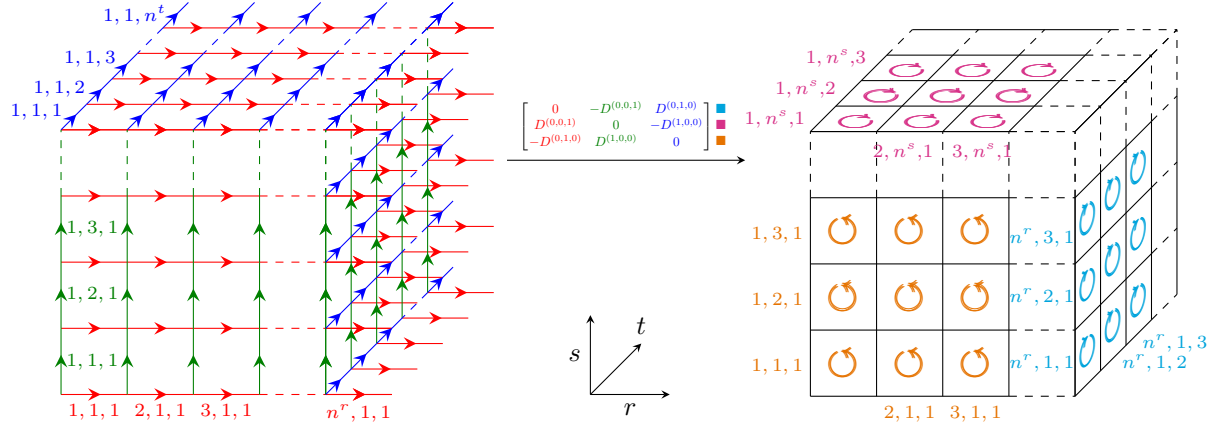


Figure 11: The action of the curl operator when associating the DOFs in  $\mathbb{S}^{p^r-1, p^s, p^t} \times \mathbb{S}^{p^r, p^s-1, p^t} \times \mathbb{S}^{p^r, p^s, p^t-1}$  to the oriented edges of a tensor mesh  $\mathcal{M}$ , as shown on the left side of the figure. In  $\mathbb{S}^{p^r, p^s-1, p^t-1} \times \mathbb{S}^{p^r-1, p^s, p^t-1} \times \mathbb{S}^{p^r-1, p^s-1, p^t}$  the DOFs become oriented faces of  $\mathcal{M}$  and the curl action on the DOFs consists in mapping the edges framing a face to such face, in this geometric interpretation. In particular, the first components of the DOFs in  $\mathbb{S}^{p^r, p^s-1, p^t-1} \times \mathbb{S}^{p^r-1, p^s, p^t-1} \times \mathbb{S}^{p^r-1, p^s-1, p^t}$  correspond to faces parallel to the  $(s, t)$ -plane, the seconds to faces parallel to the  $(r, t)$ -plane and the third components to faces parallel to the  $(r, s)$ -plane. Because of the periodicity of the spaces in the  $r$  and  $t$  directions we should have faces going outwards on the left and back sides of the tensor mesh  $\mathcal{M}$ , as we do for the edges. We have chosen to omit such faces for the readability of the figure.

and  $g_{ijk}^3$  as oriented edges in a tensor mesh  $\mathcal{M}$ . Furthermore, each collection of four edges invoked in the expressions of  $h_{ijk}^1, h_{ijk}^2$  and  $h_{ijk}^3$  frame a face of  $\mathcal{M}$ . On the other hand, the DOFs in  $\mathbb{S}^{p^r, p^s-1, p^t-1} \times \mathbb{S}^{p^r-1, p^s, p^t-1} \times \mathbb{S}^{p^r-1, p^s-1, p^t}$  are the oriented faces of  $\mathcal{M}$ , in this geometric interpretation. From this point of view, the curl operator maps the oriented edges framing a face to such face equipped with the orientation induced by the edges, as shown in Figure 11.

Let now  $g \in V_1$ ,  $g = \mathbf{N}^{(1)} \cdot \mathbf{g}$  for a set of coefficients  $\mathbf{g} = (g_1, \dots, g_{n_1})^T$ . In order to simplify the notation in what follows, let us introduce  $\bar{n}_2 = \bar{n}_0 - 3$ . We now define the action of the curl on the DOFs in  $V_1$ . We want it to mimic what we had for the DOFs in  $\mathbb{S}^{p^r-1, p^s, p^t} \times \mathbb{S}^{p^r, p^s-1, p^t} \times \mathbb{S}^{p^r, p^s, p^{t-1}}$ . If in the latter, the geometric interpretation of such action consisted in mapping the edges to the faces of a tensor mesh  $\mathcal{M}$ , this time the curl should map the edges to the faces of the polygonal ring  $\mathcal{R}$  introduced in Section 3.2, as shown in Figure 12. The total number of faces in  $\mathcal{R}$  is  $n_2 := n^t(\bar{n}_1 + \bar{n}_2)$ , as the number of faces in a joint of  $\mathcal{R}$  is  $\bar{n}_2$  and the number of faces in each side is  $\bar{n}_1$ , which is equal to the number of edges in a joint. The action on the DOFs operated by the curl is expressed by the matrix  $D^{(1)}$  of size  $n_2 \times n_1$  which, when applied to

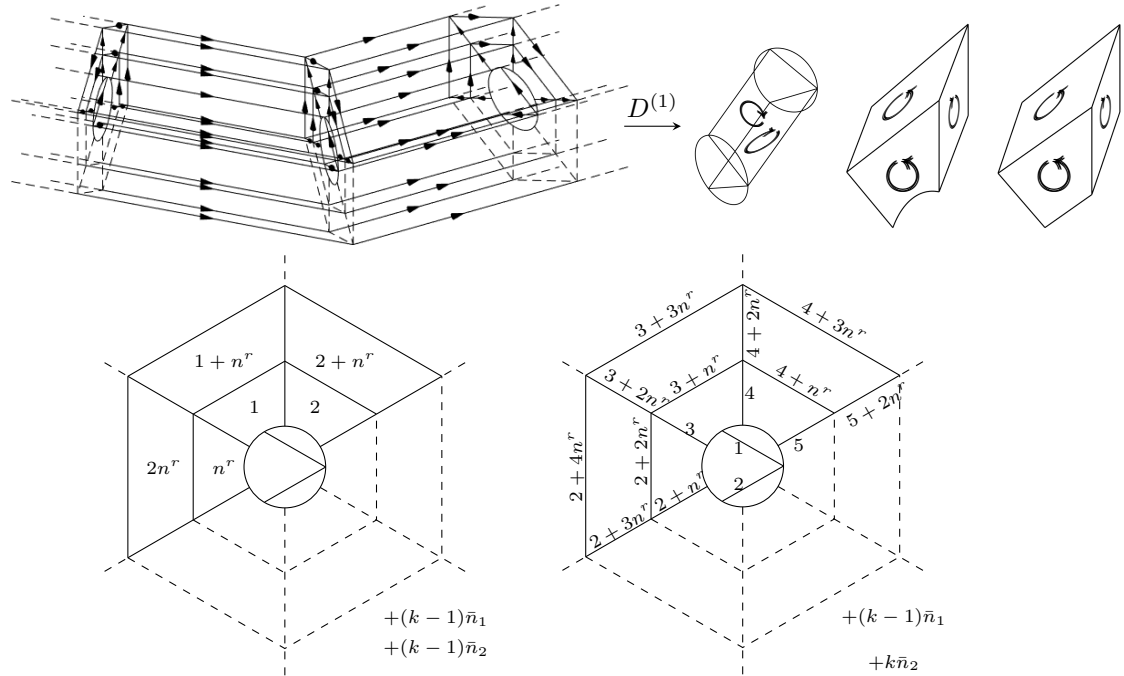


Figure 12: The action of the curl operator when associating the DOFs in  $V_1$  to the oriented edges of the polygonal ring  $\mathcal{R}$ . In the curl space the DOFs correspond to oriented faces of  $\mathcal{R}$ . On the top of the figure we see part of  $\mathcal{R}$ . In particular on the right we show sampled faces of  $\mathcal{R}$ . The left-most pair of sampled faces are those connecting the centers of two consecutive joints of  $\mathcal{R}$ .  $D^{(1)}$  is the matrix encoding the action of the curl in this geometric interpretation and maps the edges to the faces. On the bottom of the figure we see the index numbering of the DOFs in the curl space associated to the faces from the point of view of the  $k$ th joint of  $\mathcal{R}$ , for  $k \in \{1, \dots, n^t\}$ . In particular the faces between the  $k$ th joint and the  $(k+1)$ th joint are seen as edges from this prospective in the right-most figure.

$\mathbf{g}$ , produces a vector  $\mathbf{h} = D^{(1)}\mathbf{g}$  with the entries  $\{h_\ell\}_{\ell=1}^{n_2}$  given by

```

for  $k = 1, \dots, n^t$ 
  for  $i = 1, \dots, n^r - 1$ 
    
$$h_{i+(k-1)(\bar{n}_2+\bar{n}_1)} = g_{i+3+(k-1)(\bar{n}_0+\bar{n}_1)} - g_{i+2+(k-1)(\bar{n}_0+\bar{n}_1)} +$$

    
$$- g_{n^r+i+2+(k-1)(\bar{n}_0+\bar{n}_1)} + \sum_{\ell=1}^2 \bar{E}_{(\ell+1)(\Delta i, 2)} g_{\ell+(k-1)(\bar{n}_0+\bar{n}_1)};$$

    
$$h_{n^r+(k-1)(\bar{n}_2+\bar{n}_1)} = g_{3+(k-1)(\bar{n}_0+\bar{n}_1)} - g_{n^r+2+(k-1)(\bar{n}_0+\bar{n}_1)} +$$

    
$$- g_{2n^r+2+(k-1)(\bar{n}_0+\bar{n}_1)} + \sum_{\ell=1}^2 \bar{E}_{(\ell+1)(\Delta n^r, 2)} g_{\ell+(k-1)(\bar{n}_0+\bar{n}_1)};$$

  for  $j = 2, \dots, n^s - 2$ 
    for  $i = 1, \dots, n^r - 1$ 
      
$$h_{i+(j-1)n^r+(k-1)(\bar{n}_2+\bar{n}_1)} = g_{3+i+2(j-1)n^r+(k-1)(\bar{n}_0+\bar{n}_1)} - g_{2+i+2(j-1)n^r+(k-1)(\bar{n}_0+\bar{n}_1)} +$$

      
$$- g_{2+i+(2j-1)n^r+(k-1)(\bar{n}_0+\bar{n}_1)} + g_{2+i+(2j-3)n^r+(k-1)(\bar{n}_0+\bar{n}_1)};$$

      
$$h_{jn^r+(k-1)(\bar{n}_2+\bar{n}_1)} = g_{3+2(j-1)n^r+(k-1)(\bar{n}_0+\bar{n}_1)} - g_{2+(2j-1)n^r+(k-1)(\bar{n}_0+\bar{n}_1)} +$$

      
$$- g_{2+2jn^r+(k-1)(\bar{n}_0+\bar{n}_1)} + g_{2+2(j-1)n^r+(k-1)(\bar{n}_0+\bar{n}_1)};$$

    
$$h_{1+k\bar{n}_2+(k-1)\bar{n}_1} = g_{2+(k-1)\bar{n}_0+k\bar{n}_1} - g_{1+(k-1)\bar{n}_0+k\bar{n}_1} + g_{1+(k-1)(\bar{n}_0+\bar{n}_1)} - g_{1+k(\bar{n}_0+\bar{n}_1)};$$

    
$$h_{2+k\bar{n}_2+(k-1)\bar{n}_1} = g_{3+(k-1)\bar{n}_0+k\bar{n}_1} - g_{1+(k-1)\bar{n}_0+k\bar{n}_1} + g_{2+(k-1)(\bar{n}_0+\bar{n}_1)} - g_{2+k(\bar{n}_0+\bar{n}_1)};$$

    for  $i = 1, \dots, n^r$ 
      
$$h_{2+i+k\bar{n}_2+(k-1)\bar{n}_1} = -g_{i+2+k(\bar{n}_0+\bar{n}_1)} + g_{i+2+(k-1)(\bar{n}_0+\bar{n}_1)} +$$

      
$$+ g_{i+3+(k-1)\bar{n}_0+k\bar{n}_1} - \sum_{\ell=1}^3 \bar{E}_{\ell, (i, 2)} g_{\ell+(k-1)\bar{n}_0+k\bar{n}_1};$$

  for  $j = 3, \dots, n^s - 1$ 
    for  $i = 1, \dots, n^r$ 
      
$$h_{2+i+(2j-5)n^r+k\bar{n}_2+(k-1)\bar{n}_1} = -g_{i+2+(2j-5)n^r+k(\bar{n}_0+\bar{n}_1)} + g_{i+2+(2j-5)n^r+(k-1)(\bar{n}_0+\bar{n}_1)} +$$

      
$$+ g_{i+4+(j-3)n^r+(k-1)\bar{n}_0+k\bar{n}_1} - g_{i+3+(j-3)n^r+(k-1)\bar{n}_0+k\bar{n}_1};$$

      
$$h_{2+i+(2j-4)n^r+k\bar{n}_2+(k-1)\bar{n}_1} = -g_{i+2+(2j-4)n^r+k(\bar{n}_0+\bar{n}_1)} + g_{i+2+(2j-4)n^r+(k-1)(\bar{n}_0+\bar{n}_1)} +$$

      
$$+ g_{i+3+(j-2)n^r+(k-1)\bar{n}_0+k\bar{n}_1} - g_{i+3+(j-3)n^r+(k-1)\bar{n}_0+k\bar{n}_1};$$

    for  $i = 1, \dots, n^r$ 
      
$$h_{2+i+(2n^s-5)n^r+k\bar{n}_2+(k-1)\bar{n}_1} = -g_{i+2+(2n^s-5)n^r+k(\bar{n}_0+\bar{n}_1)} + g_{i+2+(2n^s-5)n^r+(k-1)(\bar{n}_0+\bar{n}_1)} +$$

      
$$+ g_{i+4+(n^s-3)n^r+(k-1)\bar{n}_0+k\bar{n}_1} - g_{i+3+(n^s-3)n^r+(k-1)\bar{n}_0+k\bar{n}_1};$$


```

with the conventions that when  $i + m = n^r + m$  we take “ $i + m = m$ ” and similarly when we have  $n^t(\bar{n}_0 + \bar{n}_1) + m$  in an index, we consider “ $n^t(\bar{n}_0 + \bar{n}_1) + m = m$ ”. Each entry of  $\mathbf{h}$  is a linear combination of four DOFs of  $V_1$  associated to edges of  $\mathcal{R}$  framing a face. The only exceptions are those entries corresponding to faces with an edge on the cylinders in the center of the sides of  $\mathcal{R}$ , i.e.,  $h_{i+(k-1)(\bar{n}_2+\bar{n}_1)}$  and  $h_{2+i+k\bar{n}_2+(k-1)\bar{n}_1}$  for  $i = 1, \dots, n^r$  and  $k = 1, \dots, n^t$ , for which we need a suitable linear combination of the edges inside such cylinders, with coefficients taken from the block  $\bar{E}$  of matrix  $E^{(0)}$  of Equation (12).

Let now  $E^{(0,1,1)}$ ,  $E^{(1,0,1)}$  and  $E^{(1,1,0)}$  be the following matrices:

$$\begin{aligned}
 E^{(0,1,1)} &:= I_{n^t} \otimes [O^{(0,1,1)}; E^{(0,1)}], \\
 E^{(1,0,1)} &:= I_{n^t} \otimes [O^{(1,0,1)}; -E^{(1,0)}], \\
 E^{(1,1,0)} &:= I_{n^t} \otimes [E^{(2)}; O^{(1,1,0)}],
 \end{aligned} \tag{24}$$

where  $O^{(0,1,1)}$ ,  $O^{(1,0,1)}$  and  $O^{(1,1,0)}$  are zero matrices of size  $\bar{n}_2 \times n^r(n^s - 1)$ ,  $\bar{n}_2 \times n^r n^s$  and  $\bar{n}_1 \times n^r(n^s - 1)$ , respectively,  $E^{(1,0)}$ ,  $E^{(0,1)}$  are the matrices of Equation (18) and  $E^{(2)}$  is the matrix, introduced in [35], of size  $\bar{n}_2 \times n^r(n^s - 1)$ , defined as

$$E^{(2)} := [O^{(2)}; I_{\bar{n}_2}]^T, \tag{25}$$

with  $O^{(2)}$  the zero matrix of size  $n^r \times \bar{n}_2$ .  $E^{(0,1,1)}$ ,  $E^{(1,0,1)}$  and  $E^{(1,1,0)}$  have sizes  $n_2 \times n^r(n^s - 1)n^t$ ,  $n_2 \times n^r n^s n^t$  and  $n_2 \times n^r(n^s - 1)n^t$ . These matrices will provide the relation between the DOFs in  $V_2$  and in

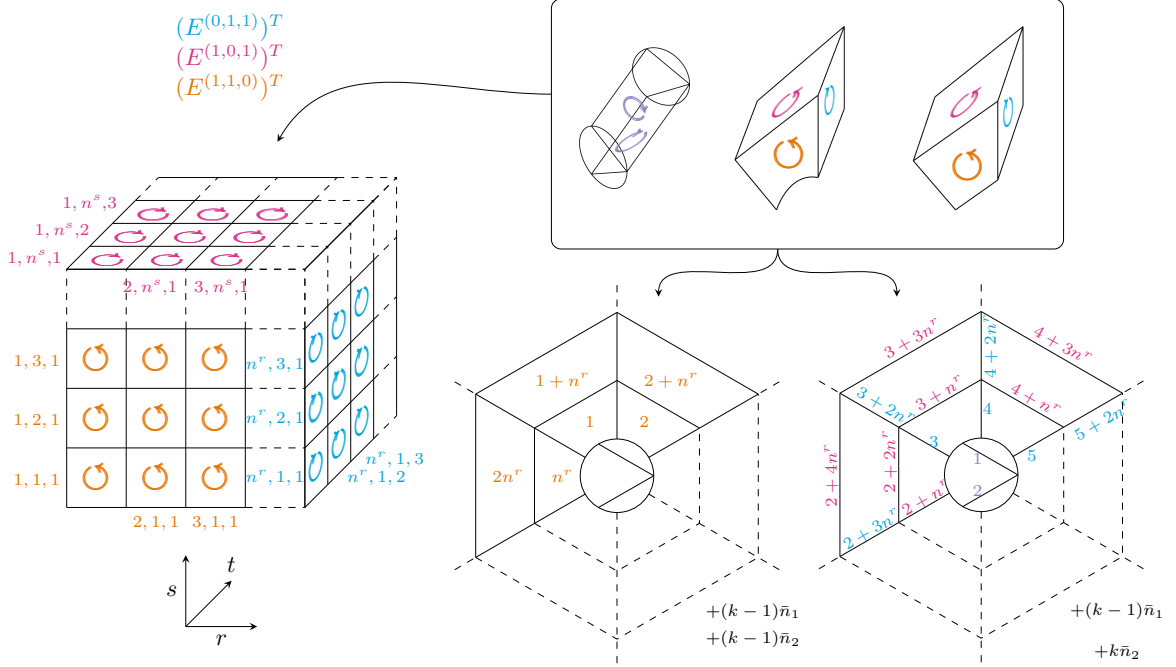


Figure 13: Geometric interpretation of the DOFs in the curl spaces  $\mathbb{S}^{p^r, p^s-1, p^t-1} \times \mathbb{S}^{p^r-1, p^s, p^t-1} \times \mathbb{S}^{p^r-1, p^s-1, p^t}$  (left) and  $V_2$  (right). In the former space, the DOFs are associated to the oriented faces of a tensor mesh  $\mathcal{M}$ . As we have already pointed out in Figure 11, there should be faces going outward of  $\mathcal{M}$  in the left and back sides because of the periodicity of the spaces. However we have omitted them for the sake of readability. In  $V_2$  instead, the DOFs are represented as oriented faces of the polygonal ring  $\mathcal{R}$  defined in Section 3.2. In the top-right part of the figure we show in a box some sampled faces of  $\mathcal{R}$ . In the middle figures we show the numbering of the faces corresponding to the DOFs in  $V_2$  from the point of view of the  $k$ th joint of  $\mathcal{R}$ , with  $k \in \{1, \dots, n^t\}$ . In particular the faces between the  $k$ th joint and the  $(k+1)$ th joint are seen as edges from this prospective. When considering a function in  $V_2$ , one can get its representation in terms of the basis functions of  $\mathbb{S}^{p^r, p^s-1, p^t-1} \times \mathbb{S}^{p^r-1, p^s, p^t-1} \times \mathbb{S}^{p^r-1, p^s-1, p^t}$  by applying the transpose of the matrices  $E^{(0,1,1)}$ ,  $E^{(1,0,1)}$  and  $E^{(1,1,0)}$  defined in (24).

$\mathbb{S}^{p^r, p^s-1, p^t-1} \times \mathbb{S}^{p^r-1, p^s, p^t-1} \times \mathbb{S}^{p^r-1, p^s-1, p^t}$ , accordingly to Remark 2.1. Namely, given a set of DOFs in  $V_2$ ,  $\mathbf{h} = \{h_\ell\}_{\ell=1}^{n_2}$ , we will have that

$$\mathbf{h}^1 = (E^{(0,1,1)})^T \mathbf{h},$$

$$\mathbf{h}^2 = (E^{(1,0,1)})^T \mathbf{h}, \quad (26)$$

$$\mathbf{h}^3 = (E^{(1,1,0)})^T \mathbf{h},$$

where  $\mathbf{h}^1, \mathbf{h}^2, \mathbf{h}^3$  are the vectorizations of the DOFs in the first, second and third components of an element  $h \in \mathbb{S}^{p^r, p^s-1, p^t-1} \times \mathbb{S}^{p^r-1, p^s, p^t-1} \times \mathbb{S}^{p^r-1, p^s-1, p^t}$ , i.e.,

$$h = \begin{pmatrix} h^1 \\ h^2 \\ h^3 \end{pmatrix} = \begin{pmatrix} \mathbf{B}^{(0,1,1)} \cdot \mathbf{h}^1 \\ \mathbf{B}^{(1,0,1)} \cdot \mathbf{h}^2 \\ \mathbf{B}^{(1,1,0)} \cdot \mathbf{h}^3 \end{pmatrix} \in \mathbb{S}^{p^r, p^s-1, p^t-1} \times \mathbb{S}^{p^r-1, p^s, p^t-1} \times \mathbb{S}^{p^r-1, p^s-1, p^t}.$$

The geometric interpretation of this link between the DOFs in  $V_2$  and in  $\mathbb{S}^{p^r, p^s-1, p^t-1} \times \mathbb{S}^{p^r-1, p^s, p^t-1} \times \mathbb{S}^{p^r-1, p^s-1, p^t}$  is visualized in Figure 13.

**Proposition 3.4.** *Let us indicate with*

- $\{g_{ijk}^1\}_{i,j,k=1}^{n^r, n^s, n^t}, \{g_{ijk}^2\}_{i,j,k=1}^{n^r, n^s-1, n^t}, \{g_{ijk}^3\}_{i,j,k=1}^{n^r, n^s, n^t}$  a general set of DOFs in  $\mathbb{S}^{p^r-1, p^s, p^t} \times \mathbb{S}^{p^r, p^s-1, p^t} \times \mathbb{S}^{p^r, p^s, p^t-1}$ ,
- $\{h_{ijk}^1\}_{i,j,k=1}^{n^r, n^s-1, n^t}, \{h_{ijk}^2\}_{i,j,k=1}^{n^r, n^s, n^t}, \{h_{ijk}^3\}_{i,j,k=1}^{n^r, n^s-1, n^t}$  a general set of DOFs in  $\text{im}(\text{curl}) \subseteq \mathbb{S}^{p^r, p^s-1, p^t-1} \times \mathbb{S}^{p^r-1, p^s, p^t-1} \times \mathbb{S}^{p^r-1, p^s-1, p^t}$ ,
- $\{g_\ell\}_{\ell=1}^{n_1}$  a general set of DOFs in  $V_1$ ,
- $\{h_\ell\}_{\ell=1}^{n_2}$  the collection of number such that Equation (26) holds true for any given choice of the DOFs  $\{h_{ijk}^1\}_{i,j,k=1}^{n^r, n^s-1, n^t}, \{h_{ijk}^2\}_{i,j,k=1}^{n^r, n^s, n^t}, \{h_{ijk}^3\}_{i,j,k=1}^{n^r, n^s-1, n^t}$ .

Then the following diagrams commute:

$$\begin{array}{ccc}
 \{g_{ijk}^1\}_{i,j,k=1}^{n^r, n^s, n^t}, \{g_{ijk}^2\}_{i,j,k=1}^{n^r, n^s-1, n^t}, \{g_{ijk}^3\}_{i,j,k=1}^{n^r, n^s, n^t} & \xrightarrow{[0 \quad -D^{(0,0,1)} \quad D^{(0,1,0)}]} & \{h_{ijk}^1\}_{i,j,k=1}^{n^r, n^s-1, n^t} \\
 \uparrow (E^{(1,0,0)})^T & \text{dashed} & \uparrow (E^{(0,1,1)})^T \\
 \uparrow (E^{(0,1,0)})^T & & \\
 \uparrow (E^{(0,0,1)})^T & & \\
 \{g_\ell\}_{\ell=1}^{n_1} & \xrightarrow{D^{(1)}} & \{h_\ell\}_{\ell=1}^{n_2} \\
 \end{array}
 \quad (a)$$

$$\begin{array}{ccc}
 \{g_{ijk}^1\}_{i,j,k=1}^{n^r, n^s, n^t}, \{g_{ijk}^2\}_{i,j,k=1}^{n^r, n^s-1, n^t}, \{g_{ijk}^3\}_{i,j,k=1}^{n^r, n^s, n^t} & \xrightarrow{[D^{(0,0,1)} \quad 0 \quad -D^{(1,0,0)}]} & \{h_{ijk}^2\}_{i,j,k=1}^{n^r, n^s, n^t} \\
 \uparrow (E^{(1,0,0)})^T & \text{dashed} & \uparrow (E^{(1,0,1)})^T \\
 \uparrow (E^{(0,1,0)})^T & & \\
 \uparrow (E^{(0,0,1)})^T & & \\
 \{g_\ell\}_{\ell=1}^{n_1} & \xrightarrow{D^{(1)}} & \{h_\ell\}_{\ell=1}^{n_2} \\
 \end{array}
 \quad (b)$$

$$\begin{array}{ccc}
 \{g_{ijk}^1\}_{i,j,k=1}^{n^r, n^s, n^t}, \{g_{ijk}^2\}_{i,j,k=1}^{n^r, n^s-1, n^t}, \{g_{ijk}^3\}_{i,j,k=1}^{n^r, n^s, n^t} & \xrightarrow{[-D^{(0,1,0)} \quad D^{(1,0,0)} \quad 0]} & \{h_{ijk}^3\}_{i,j,k=1}^{n^r, n^s-1, n^t} \\
 \uparrow (E^{(1,0,0)})^T & \text{dashed} & \uparrow (E^{(1,1,0)})^T \\
 \uparrow (E^{(0,1,0)})^T & & \\
 \uparrow (E^{(0,0,1)})^T & & \\
 \{g_\ell\}_{\ell=1}^{n_1} & \xrightarrow{D^{(1)}} & \{h_\ell\}_{\ell=1}^{n_2} \\
 \end{array}
 \quad (c)$$

*Proof.* We use an analogous argument of the proof of Proposition 3.1. In order to simplify the readability of the computations, we make use of the notations  $\bar{E}_{\ell,(\Delta i,j)}$  and  $\bar{E}_{\ell,(i,2-1)}$  introduced in Equation (20). Let

us start with diagram (a). We distinguish the cases for  $j = 1$ ,  $j = 2$  and  $j \geq 3$ . For  $j = 1$  we have

$$\begin{aligned}
h_{i1k}^1 &\stackrel{\text{curl}}{=} g_{i2k}^3 - g_{i1k}^3 + g_{i1k}^2 - g_{i1(k+1)}^2 \\
&\stackrel{(E^{(0,1,0)})^T}{=} \sum_{\ell=1}^3 \bar{E}_{\ell(i,2-1)} g_{\ell+(k-1)\bar{n}_0+k\bar{n}_1} + \sum_{\ell=1}^2 \bar{E}_{(\ell+1)(i,2-1)} (g_{\ell+(k-1)(\bar{n}_0+\bar{n}_1)} - g_{\ell+k(\bar{n}_0+\bar{n}_1)}) \\
&= \sum_{\ell=1}^2 \bar{E}_{(\ell+1)(i,2-1)} (g_{\ell+1+(k-1)\bar{n}_0+k\bar{n}_1} + g_{\ell+(k-1)(\bar{n}_0+\bar{n}_1)} - g_{\ell+k(\bar{n}_0+\bar{n}_1)}) + \bar{E}_{1(i,2-1)} g_{1+(k-1)\bar{n}_0+k\bar{n}_1} + \\
&\quad + \sum_{\ell=1}^2 \bar{E}_{(\ell+1)(i,2-1)} g_{1+(k-1)\bar{n}_0+k\bar{n}_1} - \sum_{\ell=1}^2 \bar{E}_{(\ell+1)(i,2-1)} g_{1+(k-1)\bar{n}_0+k\bar{n}_1} \\
&\stackrel{\text{DTA}}{=} \sum_{\ell=1}^2 \bar{E}_{(\ell+1)(i,2-1)} (g_{\ell+1+(k-1)\bar{n}_0+k\bar{n}_1} - g_{1+(k-1)\bar{n}_0+k\bar{n}_1} + g_{\ell+(k-1)(\bar{n}_0+\bar{n}_1)} - g_{\ell+k(\bar{n}_0+\bar{n}_1)}) \\
&\stackrel{D^{(1)}}{=} \sum_{\ell=1}^2 \bar{E}_{(\ell+1)(i,2-1)} h_{\ell+k\bar{n}_2+(k-1)\bar{n}_1} \stackrel{(E^{(0,1,1)})^T}{=} h_{i1k}^1.
\end{aligned}$$

For  $j = 2$  and  $j \geq 3$  the proof is simpler. When  $j = 2$  we have

$$\begin{aligned}
h_{i2k}^1 &\stackrel{\text{curl}}{=} g_{i3k}^3 - g_{i2k}^3 + g_{i2k}^2 - g_{i2(k+1)}^2 \\
&\stackrel{(E^{(0,1,0)})^T}{=} g_{i+3+(k-1)\bar{n}_0+k\bar{n}_1} - \sum_{\ell=1}^3 \bar{E}_{\ell(i,2)} g_{\ell+(k-1)\bar{n}_0+k\bar{n}_1} + g_{2+i+(k-1)(\bar{n}_0+\bar{n}_1)} - g_{2+i+k(\bar{n}_0+\bar{n}_1)} \\
&\stackrel{D^{(1)}}{=} h_{2+i+k\bar{n}_2+(k-1)\bar{n}_1} \stackrel{(E^{(0,1,1)})^T}{=} h_{i2k}^1,
\end{aligned}$$

while, if  $j \geq 3$  it holds

$$\begin{aligned}
h_{ijk}^1 &\stackrel{\text{curl}}{=} g_{i(j+1)k}^3 - g_{ijk}^3 + g_{ijk}^2 - g_{i(j+1)k}^2 \\
&\stackrel{(E^{(0,1,0)})^T}{=} g_{i+3+(j-2)n^r+(k-1)\bar{n}_0+k\bar{n}_1} - g_{i+3+(j-3)n^r+(k-1)\bar{n}_0+k\bar{n}_1} + \\
&\quad + g_{2+i+(2j-4)n^r+(k-1)(\bar{n}_0+\bar{n}_1)} - g_{2+i+(2j-4)n^r+k(\bar{n}_0+\bar{n}_1)} \\
&\stackrel{D^{(1)}}{=} h_{2+i+(2j-4)n^r+k\bar{n}_2+(k-1)\bar{n}_1} \stackrel{(E^{(0,1,1)})^T}{=} h_{ijk}^1.
\end{aligned}$$

This concludes the proof of commutation for diagram (a). Let us move to diagram (b). This time as well we divide the cases  $j = 1$ ,  $j = 2$  and  $j \geq 3$ . When  $j = 1$  we get

$$\begin{aligned}
h_{i1k}^2 &\stackrel{\text{curl}}{=} g_{i1(k+1)}^1 - g_{i1k}^1 + g_{i1k}^3 - g_{(i+1)1k}^3 \stackrel{(E^{(1,0,0)})^T}{=} - \sum_{\ell=1}^3 \bar{E}_{\ell(\Delta i,1)} g_{\ell+(k-1)\bar{n}_0+k\bar{n}_1} \\
&= 0 \stackrel{D^{(1)}}{=} 0 \stackrel{(E^{(1,0,1)})^T}{=} h_{i1k}^2,
\end{aligned}$$

where we have used that  $\bar{E}_{\ell,(\Delta i,1)} = 0$  for all  $i$ . If  $j = 2$ , it holds

$$\begin{aligned}
h_{i2k}^2 &\stackrel{\text{curl}}{=} g_{i2(k+1)}^1 - g_{i2k}^1 + g_{i2k}^3 - g_{(i+1)2k}^3 \\
&\stackrel{(E^{(1,0,0)})^T}{=} \sum_{\ell=1}^2 \bar{E}_{(\ell+1)(\Delta i,2)}(g_{\ell+k(\bar{n}_0+\bar{n}_1)} - g_{\ell+(k-1)(\bar{n}_0+\bar{n}_1)}) - \sum_{\ell=1}^3 \bar{E}_{\ell(\Delta i,2)}g_{\ell+(k-1)\bar{n}_0+k\bar{n}_1} \\
&= \sum_{\ell=1}^2 \bar{E}_{(\ell+1)(\Delta i,2)}(-g_{\ell+1+(k-1)\bar{n}_0+k\bar{n}_1} + g_{\ell+k(\bar{n}_0+\bar{n}_1)} - g_{\ell+(k-1)(\bar{n}_0+\bar{n}_1)}) - \bar{E}_{1(\Delta i,2)}g_{1+(k-1)\bar{n}_0+k\bar{n}_1} + \\
&\quad + \sum_{\ell=1}^2 \bar{E}_{(\ell+1)(\Delta i,2)}g_{1+(k-1)\bar{n}_0+k\bar{n}_1} - \sum_{\ell=1}^2 \bar{E}_{(\ell+1)(\Delta i,2)}g_{1+(k-1)\bar{n}_0+k\bar{n}_1} \\
&\stackrel{\text{DTA}}{=} \sum_{\ell=1}^2 \bar{E}_{(\ell+1)(\Delta i,2)}(-g_{\ell+1+(k-1)\bar{n}_0+k\bar{n}_1} + g_{1+(k-1)\bar{n}_0+k\bar{n}_1} + g_{\ell+k(\bar{n}_0+\bar{n}_1)} - g_{\ell+(k-1)(\bar{n}_0+\bar{n}_1)}) \\
&\stackrel{D^{(1)}}{=} - \sum_{\ell=1}^2 \bar{E}_{(\ell+1)(\Delta i,2)}h_{\ell+k\bar{n}_2+(k-1)\bar{n}_1} \stackrel{(E^{(1,0,1)})^T}{=} h_{i2k}^2.
\end{aligned}$$

Finally, for  $j = 3$  we have

$$\begin{aligned}
h_{ijk}^2 &\stackrel{\text{curl}}{=} g_{ij(k+1)}^1 - g_{ijk}^1 + g_{ijk}^3 - g_{(i+1)jk}^3 \\
&\stackrel{(E^{(1,0,0)})^T}{=} \begin{aligned} &g_{2+i+(2j-5)n^r+k(\bar{n}_0+\bar{n}_1)} - g_{2+i+(2j-5)n^r+(k-1)(\bar{n}_0+\bar{n}_1)} + \\ &+ g_{3+i+(j-3)n^r+(k-1)\bar{n}_0+k\bar{n}_1} - g_{4+i+(j-3)n^r+(k-1)\bar{n}_0+k\bar{n}_1} \end{aligned} \\
&\stackrel{D^{(1)}}{=} -h_{2+i+(2j-5)n^r+k\bar{n}_2+(k-1)\bar{n}_1} \stackrel{(E^{(1,0,1)})^T}{=} h_{ijk}^2.
\end{aligned}$$

This completes the proof of commutation for diagram (b). Last there is diagram (c). Again, we split the cases  $j = 1, j = 2$  and  $j \geq 3$ . When  $j = 1$  we get

$$\begin{aligned}
h_{i1k}^3 &\stackrel{\text{curl}}{=} g_{(i+1)1k}^2 - g_{i1k}^2 + g_{i1k}^1 - g_{i2k}^1 \\
&\stackrel{(E^{(1,0,0)})^T}{=} \sum_{\ell=1}^2 \bar{E}_{\ell+1(\Delta i,2-1)}g_{\ell+(k-1)(\bar{n}_0+\bar{n}_1)} - \sum_{\ell=1}^2 \bar{E}_{\ell+1(\Delta i,2)}g_{\ell+(k-1)(\bar{n}_0+\bar{n}_1)} \\
&= - \sum_{\ell=1}^2 \bar{E}_{\ell+1(\Delta i,1)}g_{\ell+(k-1)(\bar{n}_0+\bar{n}_1)} = 0 \stackrel{D^{(1)}}{=} 0 \stackrel{(E^{(1,1,0)})^T}{=} h_{i1k}^3,
\end{aligned}$$

where we have used that  $\bar{E}_{\ell,(\Delta i,1)} = 0$  for all  $i$ . If  $j = 2$ , it holds

$$\begin{aligned}
h_{i2k}^3 &\stackrel{\text{curl}}{=} g_{(i+1)2k}^2 - g_{i2k}^2 + g_{i2k}^1 - g_{i3k}^1 \\
&\stackrel{(E^{(1,0,0)})^T}{=} g_{3+i+(k-1)(\bar{n}_0+\bar{n}_1)} - g_{2+i+(k-1)(\bar{n}_0+\bar{n}_1)} + \sum_{\ell=1}^2 \bar{E}_{\ell+1(\Delta i,2)}g_{\ell+(k-1)(\bar{n}_0+\bar{n}_1)} - g_{2+i+n^r+(k-1)(\bar{n}_0+\bar{n}_1)} \\
&\stackrel{D^{(1)}}{=} h_{i+(k-1)(\bar{n}_2+\bar{n}_1)} \stackrel{(E^{(1,1,0)})^T}{=} h_{i2k}^3.
\end{aligned}$$

Finally, for  $j \geq 3$  we have

$$\begin{aligned}
h_{ijk}^3 &\stackrel{\text{curl}}{=} g_{(i+1)jk}^2 - g_{ijk}^2 + g_{ijk}^1 - g_{i(j+1)k}^1 \\
&\stackrel{(E^{(1,0,0)})^T}{=} g_{3+i+(2j-4)n^r+(k-1)(\bar{n}_0+\bar{n}_1)} - g_{2+i+(2j-4)n^r+(k-1)(\bar{n}_0+\bar{n}_1)} + \\
&\quad + g_{2+i+(2j-5)n^r+(k-1)(\bar{n}_0+\bar{n}_1)} - g_{2+i+(2j-3)n^r+(k-1)(\bar{n}_0+\bar{n}_1)} \\
&\stackrel{D^{(1)}}{=} h_{i+(j-2)n^r+(k-1)(\bar{n}_2+\bar{n}_1)} \stackrel{(E^{(1,1,0)})^T}{=} h_{ijk}^3.
\end{aligned}$$

□

We can move to the definitions of  $V_2$  and of the extraction operator  $\mathcal{E}^2$ . We introduce the following collections of  $n_2$  functions,

$$\begin{aligned}
\mathbf{N}^{(0,1,1)} &:= E^{(0,1,1)} \mathbf{B}^{(0,1,1)}, \\
\mathbf{N}^{(1,0,1)} &:= E^{(1,0,1)} \mathbf{B}^{(1,0,1)}, \\
\mathbf{N}^{(1,1,0)} &:= E^{(1,1,0)} \mathbf{B}^{(1,1,0)}.
\end{aligned} \tag{27}$$

By looking at the structure of  $E^{(0,1,1)}$ ,  $E^{(1,0,1)}$  and  $E^{(1,1,0)}$ , reported in Equation (24), one easily recognizes that there are zero functions in  $\mathbf{N}^{(0,1,1)}$ ,  $\mathbf{N}^{(1,0,1)}$  and  $\mathbf{N}^{(1,1,0)}$ . However, there exists no index  $\ell$  in  $\{1, \dots, n_2\}$  such that  $N_\ell^{(0,1,1)}$ ,  $N_\ell^{(1,0,1)}$  and  $N_\ell^{(1,1,0)}$  are all zero. Furthermore, by using an analogous argument of the proof of Proposition 3.2, one shows the independence of the non-zero functions.

**Proposition 3.5.** *The non-zero functions in  $\mathbf{N}^{(0,1,1)}$ ,  $\mathbf{N}^{(1,0,1)}$  and  $\mathbf{N}^{(1,1,0)}$ , defined in Equation (27), are linearly independent.*

We define the space  $V_2$  as the span of the following linearly independent vector functions

$$N_\ell^{(2)} := \begin{pmatrix} N_\ell^{(0,1,1)} \\ N_\ell^{(1,0,1)} \\ N_\ell^{(1,1,0)} \end{pmatrix} \quad \text{for } \ell = 1, \dots, n_2. \tag{28}$$

The extraction operator  $\mathcal{E}^2 : \mathbb{S}^{p^r, p^s-1, p^t-1} \times \mathbb{S}^{p^r-1, p^s, p^t-1} \times \mathbb{S}^{p^r-1, p^s-1, p^t} \rightarrow V_2$  constitutes the collection  $\mathbf{N}^{(2)}$  of the functions reported in Equation (28) from the three sets of splines  $\mathbf{B}^{(0,1,1)}$ ,  $\mathbf{B}^{(1,0,1)}$  and  $\mathbf{B}^{(1,1,0)}$ . Thanks to Remark 2.1, Proposition 3.4 proves the commutation of the extraction operators  $\mathcal{E}^1$  and  $\mathcal{E}^2$  with the curl.

**Corollary 3.6.** *The diagram*

$$\begin{array}{ccccc}
\mathbb{S}^{p^r-1, p^s, p^t} \times \mathbb{S}^{p^r, p^s-1, p^t} \times \mathbb{S}^{p^r, p^s, p^t-1} & \xrightarrow{\text{curl}} & \mathbb{S}^{p^r, p^s-1, p^t-1} \times \mathbb{S}^{p^r-1, p^s, p^t-1} \times \mathbb{S}^{p^r-1, p^s-1, p^t} \\
\mathcal{E}^1 \downarrow \searrow & \xrightarrow{\text{curl}} & \downarrow \mathcal{E}^2 \\
V_1 & \xrightarrow{\text{curl}} & V_2
\end{array}$$

commutes and the pushforward of the functions in  $V_2$ , namely  $\mathcal{F}^2(N_\ell^{(2)})$  for  $\ell = 1, \dots, n_2$ , with the operator  $\mathcal{F}^2$  defined as in (8), are  $C^0$  on  $\Omega^{pol}$ .

Corollary 3.6 can be proved adapting the arguments used in the proof of Corollary 3.3.

Hence, given a function  $g \in V_1$ ,  $g = \mathbf{N}^{(1)} \cdot \mathbf{g}$ , we have the following representation of  $\operatorname{curl} g$  in terms of the basis of  $V_2$ :

$$\operatorname{curl} g = \mathbf{N}^{(2)} \cdot D^{(1)} \mathbf{g} = \begin{pmatrix} \mathbf{N}^{(0,1,1)} \cdot D^{(1)} \mathbf{g} \\ \mathbf{N}^{(1,0,1)} \cdot D^{(1)} \mathbf{g} \\ \mathbf{N}^{(1,1,0)} \cdot D^{(1)} \mathbf{g} \end{pmatrix} \in V_2.$$

### 3.5. The divergence of functions in $V_2$ , the operator $\mathcal{E}^3$ and the space $V_3$

Let  $h \in \mathbb{S}^{p^r, p^s-1, p^t-1} \times \mathbb{S}^{p^r-1, p^s, p^t-1} \times \mathbb{S}^{p^r-1, p^s-1, p^t}$ ,

$$h = \begin{pmatrix} h^1 \\ h^2 \\ h^3 \end{pmatrix} = \begin{pmatrix} \mathbf{B}^{(0,1,1)} \cdot \mathbf{h}^1 \\ \mathbf{B}^{(1,0,1)} \cdot \mathbf{h}^2 \\ \mathbf{B}^{(1,1,0)} \cdot \mathbf{h}^3 \end{pmatrix}$$

with  $\mathbf{h}^1, \mathbf{h}^2, \mathbf{h}^3$  the vectorizations of the coefficients  $\{h_{ijk}^1\}_{i,j,k=1}^{n^r, n^s-1, n^t}$ ,  $\{h_{ijk}^2\}_{i,j,k=1}^{n^r, n^s, n^t}$  and  $\{h_{ijk}^3\}_{i,j,k=1}^{n^r, n^s-1, n^t}$  obtained by running the indices first on  $i$ , then on  $j$  and then on  $k$ . The divergence of  $h$  has the following expression:

$$\operatorname{div} h = \sum_{k=1}^{n^t} \sum_{j=1}^{n^s-1} \sum_{i=1}^{n^r} (h_{(i+1)jk}^1 - h_{ijk}^1 + h_{i(j+1)k}^2 - h_{ijk}^2 + h_{ij(k+1)}^3 - h_{ijk}^3) D_i^{p^r} D_j^{p^s} D_k^{p^t}$$

where the functions  $D_i^{p^r}, D_j^{p^s}$  and  $D_k^{p^t}$  for any  $i, j, k$  have been introduced in Section 2.1. Let  $\mathbf{B}^{(1,1,1)}$  be the vectorization of  $\{D_i^{p^r} D_j^{p^s} D_k^{p^t}\}_{i,j,k=1}^{n^r, n^s-1, n^t}$ . The divergence operator  $\operatorname{div} : \mathbb{S}^{p^r, p^s-1, p^t-1} \times \mathbb{S}^{p^r-1, p^s, p^t-1} \times \mathbb{S}^{p^r-1, p^s-1, p^t} \rightarrow \mathbb{S}^{p^r-1, p^s-1, p^t-1}$  has the following matrix representation:

$$\operatorname{div} h = \mathbf{B}^{(1,1,1)} \cdot [D^{(1,0,0)} \mathbf{h}^1 + D^{(0,1,0)} \mathbf{h}^2 + D^{(0,0,1)} \mathbf{h}^3] \quad \forall h \in \mathbb{S}^{p^r, p^s-1, p^t-1} \times \mathbb{S}^{p^r-1, p^s, p^t-1} \times \mathbb{S}^{p^r-1, p^s-1, p^t},$$

where the matrices  $D^{(1,0,0)}, D^{(0,1,0)}$  and  $D^{(0,0,1)}$  have been defined in Equation (14). The DOFs in  $\operatorname{im}(\operatorname{div})$  have form

$$m_{ijk} := h_{(i+1)jk}^1 - h_{ijk}^1 + h_{i(j+1)k}^2 - h_{ijk}^2 + h_{ij(k+1)}^3 - h_{ijk}^3,$$

for  $i = 1, \dots, n^r$ ,  $j = 1, \dots, n^s - 1$  and  $k = 1, \dots, n^t$ , for some set of DOFs  $\{h_{ijk}^1\}_{i,j,k=1}^{n^r, n^s-1, n^t}$ ,  $\{h_{ijk}^2\}_{i,j,k=1}^{n^r, n^s, n^t}$ ,  $\{h_{ijk}^3\}_{i,j,k=1}^{n^r, n^s-1, n^t}$  in  $\mathbb{S}^{p^r, p^s-1, p^t-1} \times \mathbb{S}^{p^r-1, p^s, p^t-1} \times \mathbb{S}^{p^r-1, p^s-1, p^t}$ . In the geometric interpretation proposed in Section 3.2,  $h_{ijk}^1, h_{(i+1)jk}^1, h_{ijk}^2, h_{i(j+1)k}^2, h_{ijk}^3, h_{ij(k+1)}^3$  correspond to the faces of a tensor mesh  $\mathcal{M}$  enclosing the volume related to  $m_{ijk}$ . Therefore, from this geometric point of view, the divergence operator maps oriented faces enclosing a volume to such volume, as shown in Figure 14.

We want the same action onto the DOFs of  $V_2$ . This time the latter are associated to the oriented faces of the polygonal ring  $\mathcal{R}$  defined in Section 3.2. When applying the divergence operator, we should map such faces to the volumes they enclose as shown in Figure 15. The total number of volumes in  $\mathcal{R}$  is  $n_3 = n^t \bar{n}_2$ , as each face in a joint of  $\mathcal{R}$  corresponds to a volume in the side between such joint and the next joint. Given  $h \in V_2$ ,  $h = \mathbf{N}^{(2)} \cdot \mathbf{h}$  for a set of coefficients  $\mathbf{h} = (h_1, \dots, h_{n_2})^T$ , the action of the divergence on the DOFs is expressed by the matrix  $D^{(2)}$  of size  $n_3 \times n_2$  which, when applied to  $\mathbf{h}$ , produces a vector  $\mathbf{m} = D^{(2)} \mathbf{h}$  with the entries  $\{m_\ell\}_{\ell=1}^{n_3}$  given by

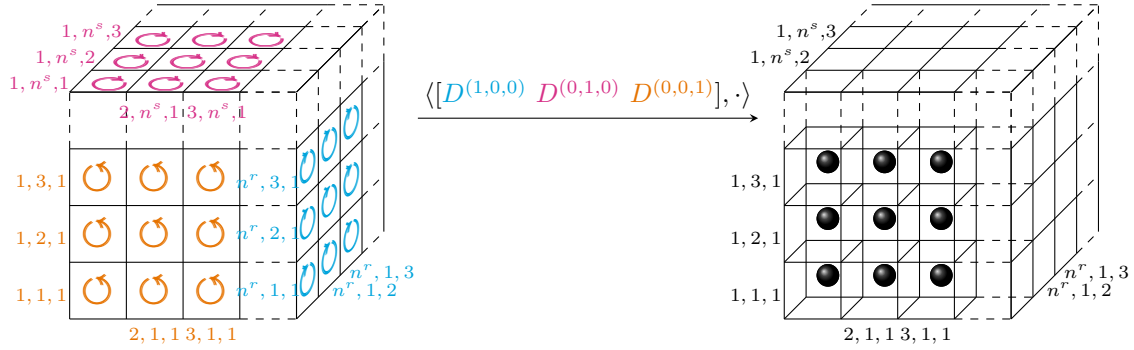


Figure 14: The action of the divergence operator when associating the DOFs in  $\mathbb{S}^{p^r, p^s-1, p^t-1} \times \mathbb{S}^{p^r-1, p^s, p^t-1} \times \mathbb{S}^{p^r-1, p^s-1, p^t}$  to the oriented faces of a tensor mesh  $\mathcal{M}$ , as shown on the left side of the figure. In this geometric interpretation, the divergence maps the six faces enclosing a volume in  $\mathcal{M}$  to such volume. For the periodicity of the spaces in the  $r$  and  $t$  directions, on the left and back sides of the tensor meshes shown in the figure there should be faces going outward, in the mesh on the left, and an extra block of volume in each side, in the mesh on the right. We have chosen to omit them for the sake of readability of the figure.

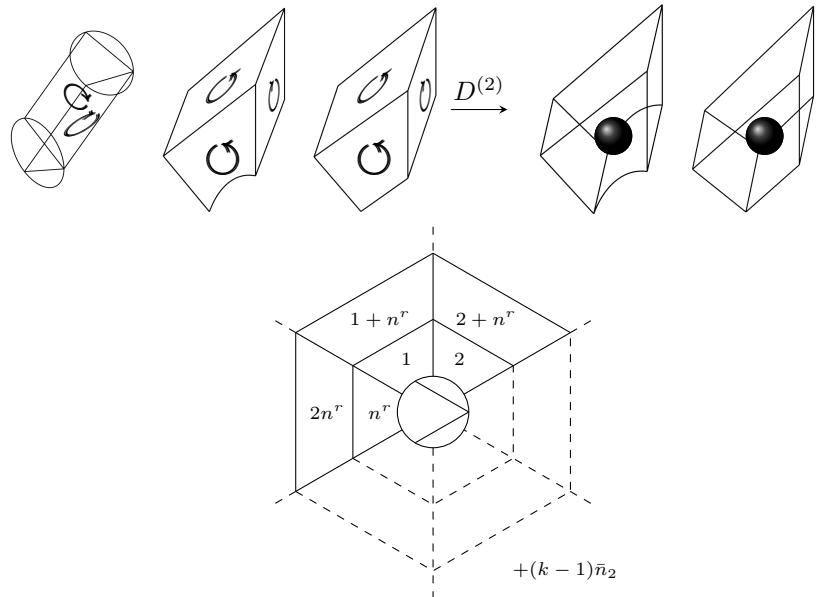


Figure 15: The action of the divergence operator when associating the DOFs in  $V_2$  to the oriented faces of the polygonal ring  $\mathcal{R}$ . In the divergence space the DOFs correspond to the volumes in  $\mathcal{R}$ . For the sake of readability, in the upper part of the figure we only show the different types of faces and volumes.  $D^{(2)}$  is the matrix encoding the action of the divergence on the DOFs and it maps the faces enclosing a volume to such volume, in this geometric interpretation. On the bottom of the figure we see the index numbering of the DOFs in the divergence space, associated to the volumes, from the point of view of the  $k$ th joint of  $\mathcal{R}$ , for  $k \in \{1, \dots, n^t\}$ . Each volume is seen as a face from this prospective.

```

for  $k = 1, \dots, n^t$ 
  for  $i = 1, \dots, n^r - 1$ 
     $m_{i+(k-1)\bar{n}_2} = h_{3+i+k\bar{n}_2+(k-1)\bar{n}_1} - h_{2+i+k\bar{n}_2+(k-1)\bar{n}_1} - h_{2+i+n^r+k\bar{n}_2+(k-1)\bar{n}_1} +$ 
     $+ \sum_{\ell=1}^2 \bar{E}_{(\ell+1)(\Delta i, 2)} h_{\ell+k\bar{n}_2+(k-1)\bar{n}_1} + h_{i+k(\bar{n}_2+\bar{n}_1)} - h_{i+(k-1)(\bar{n}_2+\bar{n}_1)};$ 
     $m_{n^r+(k-1)\bar{n}_2} = h_{3+k\bar{n}_2+(k-1)\bar{n}_1} - h_{2+n^r+k\bar{n}_2+(k-1)\bar{n}_1} - h_{2+2n^r+k\bar{n}_2+(k-1)\bar{n}_1} +$ 
     $+ \sum_{\ell=1}^2 \bar{E}_{(\ell+1)(\Delta n^r, 2)} h_{\ell+k\bar{n}_2+(k-1)\bar{n}_1} + h_{n^r+k(\bar{n}_2+\bar{n}_1)} - h_{n^r+(k-1)(\bar{n}_2+\bar{n}_1)};$ 
  for  $j = 2, \dots, n^s - 2$ 
    for  $i = 1, \dots, n^r - 1$ 
       $m_{i+(j-1)n^r+(k-1)\bar{n}_2} = h_{3+i+(2j-2)n^r+k\bar{n}_2+(k-1)\bar{n}_1} - h_{2+i+(2j-2)n^r+k\bar{n}_2+(k-1)\bar{n}_1} +$ 
       $- h_{2+i+(2j-1)n^r+k\bar{n}_2+(k-1)\bar{n}_1} + h_{2+i+(2j-3)n^r+k\bar{n}_2+(k-1)\bar{n}_1} +$ 
       $+ h_{i+(j-1)n^r+k(\bar{n}_2+\bar{n}_1)} - h_{i+(j-1)n^r+(k-1)(\bar{n}_2+\bar{n}_1)};$ 
       $m_{jn^r+(k-1)\bar{n}_2} = h_{3+(2j-2)n^r+k\bar{n}_2+(k-1)\bar{n}_1} - h_{2+(2j-1)n^r+k\bar{n}_2+(k-1)\bar{n}_1} +$ 
       $- h_{2+2jn^r+k\bar{n}_2+(k-1)\bar{n}_1} + h_{2+(2j-2)n^r+k\bar{n}_2+(k-1)\bar{n}_1} +$ 
       $+ h_{n^r+(j-1)n^r+k(\bar{n}_2+\bar{n}_1)} - h_{n^r+(j-1)n^r+(k-1)(\bar{n}_2+\bar{n}_1)};$ 

```

where we have used the notation  $\bar{E}_{\ell, (\Delta i, 2)}$  introduced in Equation (20) and the conventions “ $i + q = q$ ” when  $i = n^r$  and “ $k(\bar{n}_0 + \bar{n}_1) + q = q$ ” when  $k = n^t$ . Each entry of  $\mathbf{m}$  is expressed as linear combination of six DOFs in  $V_2$  associated to faces enclosing a volume in  $\mathcal{R}$ . The only exceptions are those entries corresponding to volumes with a boundary face on the cylinders in the center of the sides of  $\mathcal{R}$ , i.e.,  $m_{i+(k-1)\bar{n}_2}$  for  $i = 1, \dots, n^r$  and  $k = 1, \dots, n^t$ , for which we need a suitable linear combination of the two faces inside such cylinders, with coefficients taken from the block  $\bar{E}$  of matrix  $E^{(0)}$  of Equation (12).

Let now

$$E^{(1,1,1)} = I_{n^t} \otimes E^{(2)}, \quad (29)$$

where  $E^{(2)}$  is the matrix defined in Equation (25).  $E^{(1,1,1)}$  has dimension  $n_3 \times n^r(n^s - 1)n^t$  and it will provide the relation between the DOFs in  $V_3$  and  $\mathbb{S}^{p^r-1, p^s-1, p^t-1}$ , accordingly to Remark 2.1, that is, given a set of DOFs in  $V_3$ ,  $\mathbf{m} = \{m_\ell\}_{\ell=1}^{n_3}$ , we shall show that

$$\bar{\mathbf{m}} = (E^{(1,1,1)})^T \mathbf{m}, \quad (30)$$

where  $\bar{\mathbf{m}}$  is the vectorization of the DOFs of an element  $\bar{m} \in \mathbb{S}^{p^r-1, p^s-1, p^t-1}$ , i.e.,  $\bar{m} = \mathbf{B}^{(1,1,1)} \cdot \bar{\mathbf{m}}$ . The geometric interpretation of this link between the DOFs in  $V_3$  and in  $\mathbb{S}^{p^r-1, p^s-1, p^t-1}$  is shown in Figure 16.

**Proposition 3.7.** *Let us indicate with*

- $\{h_{ijk}^1\}_{i,j,k=1}^{n^r, n^s-1, n^t}, \{h_{ijk}^2\}_{i,j,k=1}^{n^r, n^s, n^t}, \{h_{ijk}^3\}_{i,j,k=1}^{n^r, n^s-1, n^t}$  a general set of DOFs in  $\mathbb{S}^{p^r, p^s-1, p^t-1} \times \mathbb{S}^{p^r-1, p^s, p^t-1} \times \mathbb{S}^{p^r-1, p^s-1, p^t}$ ,
- $\{\bar{m}_{ijk}\}_{i,j,k=1}^{n^r, n^s-1, n^t}$  a general set of DOFs in  $\text{im}(\text{div}) \subseteq \mathbb{S}^{p^r-1, p^s-1, p^t-1}$ ,
- $\{h_\ell\}_{\ell=1}^{n_2}$  a general set of DOFs in  $V_2$ ,
- $\{m_\ell\}_{\ell=1}^{n_3}$  the collection of numbers such that Equation (30) holds true for any given choice of the DOFs  $\{\bar{m}_{ijk}\}_{i,j,k=1}^{n^r, n^s-1, n^t}$ .

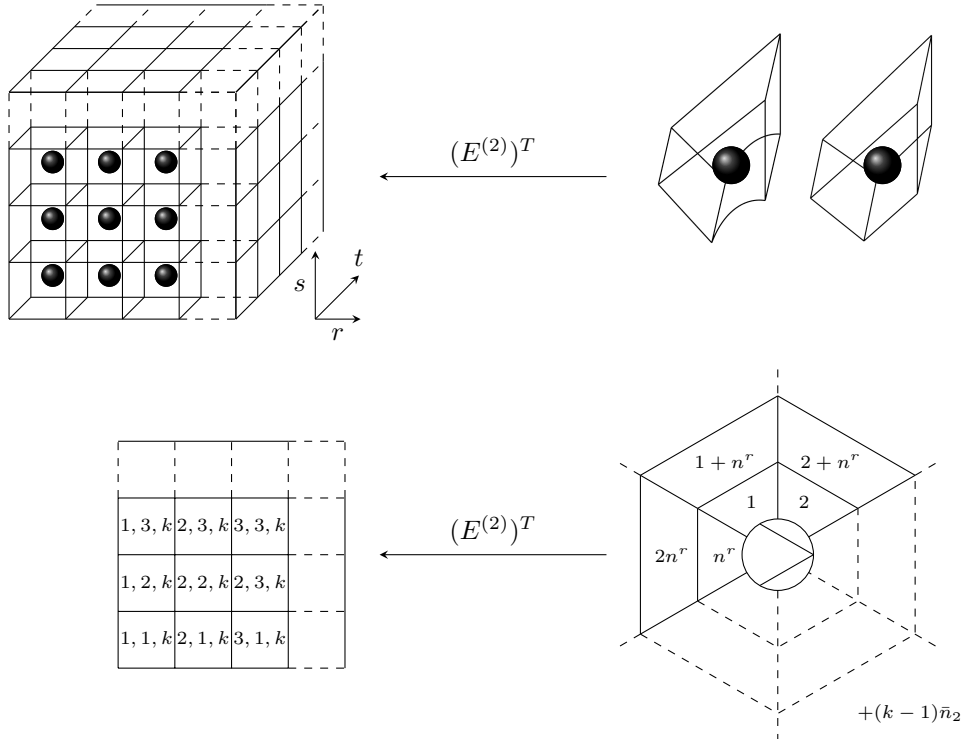


Figure 16: Geometric interpretation of the DOFs in  $\mathbb{S}^{p^{r-1}, p^s-1, p^t-1}$  (left) and  $V_3$  (right) as volumes enclosed, respectively, in a tensor mesh  $\mathcal{M}$  and a polygonal ring  $\mathcal{R}$ , as introduced in Section 3.2. On the top-right part of the figure we show the two types of volumes that can be found in  $\mathcal{R}$ . On the bottom-right part of the figure we show the indices of the DOFs corresponding to the volumes in the  $k$ th side of  $\mathcal{R}$ , seen from the point of view of the  $k$ th joint of  $\mathcal{R}$ , for  $k \in \{1, \dots, n^t\}$ . On the bottom-left we show the indices of the relative DOFs in  $\mathbb{S}^{p^{r-1}, p^s-1, p^t-1}$ , once one applies the transpose of matrix  $E^{(2)}$ , as explained in Remark 2.1. In this geometric interpretation, these latter DOFs form a slice of the mesh  $\mathcal{M}$  obtained by cutting along the  $(r, s)$ -plane.

Then the following diagram commutes:

$$\begin{array}{ccc}
\{h_{ijk}^1\}_{i,j,k=1}^{n^r, n^s-1, n^t}, \{h_{ijk}^2\}_{i,j,k=1}^{n^r, n^s, n^t}, \{h_{ijk}^3\}_{i,j,k=1}^{n^r, n^s-1, n^t} & \xrightarrow{\langle [D^{(1,0,0)}, D^{(0,1,0)}, D^{(0,0,1)}], \cdot \rangle} & \{\bar{m}_{ijk}\}_{i,j,k=1}^{n^r, n^s-1, n^t} \\
\uparrow (E^{(0,1,1)})^T & \text{dashed} & \uparrow (E^{(1,1,1)})^T \\
\uparrow (E^{(1,0,1)})^T & & \\
\uparrow (E^{(1,1,0)})^T & & \\
\{h_\ell\}_{\ell=1}^{n_2} & \xrightarrow{D^{(2)}} & \{m_\ell\}_{\ell=1}^{n_3}
\end{array}$$

*Proof.* The argument of the proof is analogous to the ones used in Propositions 3.1 and 3.4. Recalling the notations  $\bar{E}_{\ell,(\Delta i,j)}$  and  $\bar{E}_{\ell,(i,2-1)}$  introduced in Equation (20), let us define

$$\bar{E}_{\ell,(\Delta i,2-1)} := \bar{E}_{\ell,(\Delta i,2)} - \bar{E}_{\ell,(\Delta i,1)},$$

for any  $\ell = 1, 2, 3$  and  $i = 1, \dots, n^r$ . We distinguish three cases:  $j = 1$ ,  $j = 2$  and  $j \geq 3$ . For  $j = 1$  we have

$$\begin{aligned}
\bar{m}_{i1k} &\stackrel{\text{div}}{=} h_{(i+1)1k}^1 - h_{i1k}^1 + h_{i2k}^2 - h_{i1k}^2 + h_{i1(k+1)}^3 - h_{i1k}^3 \\
&\stackrel{(E^{(0,1,1)})^T}{=} \sum_{\ell=1}^2 \bar{E}_{(\ell+1)(\Delta i,2-1)} h_{\ell+k\bar{n}_2+(k-1)\bar{n}_1} - \sum_{\ell=1}^2 \bar{E}_{(\ell+1)(\Delta i,2)} h_{\ell+k\bar{n}_2+(k-1)\bar{n}_1} \\
&= - \sum_{\ell=1}^2 \bar{E}_{(\ell+1)(\Delta i,1)} h_{\ell+k\bar{n}_2+(k-1)\bar{n}_1} = 0 \stackrel{D^{(2)}}{=} 0 \stackrel{(E^{(1,1,1)})^T}{=} \bar{m}_{i1k}.
\end{aligned}$$

When  $j = 2$  it holds

$$\begin{aligned}
\bar{m}_{i2k} &\stackrel{\text{div}}{=} h_{(i+1)2k}^1 - h_{i2k}^1 + h_{i3k}^2 - h_{i2k}^2 + h_{i2(k+1)}^3 - h_{i2k}^3 \\
&\stackrel{(E^{(0,1,1)})^T}{=} h_{3+i+k\bar{n}_2+(k-1)\bar{n}_1} - h_{2+i+k\bar{n}_2+(k-1)\bar{n}_1} - h_{2+i+n^r+k\bar{n}_2+(k-1)\bar{n}_1} + \\
&\quad + \sum_{\ell=1}^2 \bar{E}_{(\ell+1)(\Delta i,2)} h_{\ell+k\bar{n}_2+(k-1)\bar{n}_1} + h_{i+k(\bar{n}_2+\bar{n}_1)} - h_{i+(k-1)(\bar{n}_2+\bar{n}_1)} \\
&\stackrel{D^{(2)}}{=} m_{i+(k-1)\bar{n}_2} \stackrel{(E^{(1,1,1)})^T}{=} \bar{m}_{i2k}.
\end{aligned}$$

Finally, for  $j \geq 3$  we get

$$\begin{aligned}
\bar{m}_{ijk} &\stackrel{\text{div}}{=} h_{(i+1)jk}^1 - h_{ijk}^1 + h_{i(j+1)k}^2 - h_{ijk}^2 + h_{ij(k+1)}^3 - h_{ijk}^3 \\
&\stackrel{(E^{(0,1,1)})^T}{=} h_{i+3+(2j-4)n^r+k\bar{n}_2+(k-1)\bar{n}_1} - h_{i+2+(2j-4)n^r+k\bar{n}_2+(k-1)\bar{n}_1} - h_{i+2+(2j-3)n^r+k\bar{n}_2+(k-1)\bar{n}_1} + \\
&\quad + h_{i+2+(2j-5)n^r+k\bar{n}_2+(k-1)\bar{n}_1} + h_{i+(j-2)n^r+k(\bar{n}_2+\bar{n}_1)} - h_{i+(j-2)n^r+(k-1)(\bar{n}_2+\bar{n}_1)} \\
&\stackrel{D^{(2)}}{=} m_{i+(j-2)n^r+(k-1)\bar{n}_2} \stackrel{(E^{(1,1,1)})^T}{=} \bar{m}_{ijk}.
\end{aligned}$$

□

Let now  $\mathbf{N}^{(3)} := E^{(1,1,1)} \mathbf{B}^{(1,1,1)}$ . By looking at Equation (29), we note that there are only non-zero functions in  $\mathbf{N}^{(3)}$  as  $E^{(1,1,1)}$  has only non-zero rows. Furthermore, such functions are linearly independent as the functions in  $\mathbf{B}^{(1,1,1)}$  are linearly independent and  $E^{(1,1,1)}$  has full rank (equal to the number of rows). We define the space  $V_3$  as the span of the functions in  $\mathbf{N}^{(3)}$ . The extraction operator  $\mathcal{E}^3 : \mathbb{S}^{p^r-1, p^s-1, p^t-1} \rightarrow V_3$  constitutes the collection of splines in  $\mathbf{N}^{(3)}$  from the spline set  $\mathbf{B}^{(1,1,1)}$ . Thanks to Remark 2.1 and Proposition 3.7, we are able to prove the following corollary.

**Corollary 3.8.** *The diagram*

$$\begin{array}{ccccc}
 \mathbb{S}^{p^r, p^s-1, p^t-1} \times \mathbb{S}^{p^r-1, p^s, p^t-1} \times \mathbb{S}^{p^r-1, p^s-1, p^t} & \xrightarrow{\text{div}} & \mathbb{S}^{p^r-1, p^s-1, p^t-1} & & \\
 \mathcal{E}^2 \downarrow & \searrow & \downarrow \mathcal{E}^3 & & \\
 V_2 & \xrightarrow{\text{div}} & V_3 & & 
 \end{array}$$

commutes and the pushforward of the functions in  $V_3$ , namely  $\mathcal{F}^3(N_\ell^{(3)})$  for  $\ell = 1, \dots, n_3$ , with the operator  $\mathcal{F}^3$  defined as in (8), are bounded on  $\Omega^{\text{pol}}$ .

Corollary 3.8 can be proved adapting the arguments used in the proof of Corollary 3.3. In particular, given a function  $h \in V_2$ ,  $h = \mathbf{N}^{(2)} \cdot \mathbf{h}$ , then  $\text{div } h = \mathbf{N}^{(3)} \cdot D^{(2)} \mathbf{h}$ .

#### 4. Preservation of the cohomology dimensions

Let us define the following spline complex on  $\Omega$ :

$$\mathfrak{S} : 0 \xrightarrow{\text{id}} V_0 \xrightarrow{\text{grad}} V_1 \xrightarrow{\text{curl}} V_2 \xrightarrow{\text{div}} V_3 \xrightarrow{0} 0. \quad (31)$$

We now prove that the cohomological structure of  $\mathfrak{S}$  is equal to the cohomological structure of (1). This preservation property will be immediately transferred to the corresponding complex on the physical domain, as we will show after the theorem.

**Theorem 4.1.** *the cohomology spaces of the spline complex  $\mathfrak{S}$  defined in Equation (31) have the following dimensions:*

$$\dim \mathcal{H}^0(\mathfrak{S}) = 1, \quad \dim \mathcal{H}^1(\mathfrak{S}) = 1, \quad \dim \mathcal{H}^2(\mathfrak{S}) = 0, \quad \dim \mathcal{H}^3(\mathfrak{S}) = 0.$$

*Proof.* Let us start by computing  $\dim \mathcal{H}^0(\mathfrak{S})$ . We know that  $\mathcal{H}^0(\mathfrak{S}) = \ker(\text{grad})$ . Let  $f \in V_0$  be such that  $\text{grad } f = 0$ . Since  $\text{grad } f = \sum_{\ell=1}^{n_1} g_\ell N_\ell^{(1)}$ , this means that the coefficients  $g_\ell = 0$  for all  $\ell$ . With reference to Equation (16), we have

$$\begin{cases} g_{1+(k-1)(\bar{n}_0+\bar{n}_1)} = f_{2+(k-1)\bar{n}_0} - f_{1+(k-1)\bar{n}_0} = 0 \\ g_{2+(k-1)(\bar{n}_0+\bar{n}_1)} = f_{3+(k-1)\bar{n}_0} - f_{1+(k-1)\bar{n}_0} = 0 \end{cases} \Rightarrow f_{1+(k-1)\bar{n}_0} = f_{2+(k-1)\bar{n}_0} = f_{3+(k-1)\bar{n}_0} = \alpha_k$$

for some  $\alpha_k \in \mathbb{R}$ . Then, for any  $i \in \{1, \dots, n^r\}$  we have

$$g_{i+2+(k-1)(\bar{n}_0+\bar{n}_1)} = f_{3+i+(k-1)\bar{n}_0} - \sum_{\ell=1}^3 \bar{E}_{\ell,(i,2)} f_{\ell+(k-1)\bar{n}_0} = 0 \Rightarrow f_{3+i+(k-1)\bar{n}_0} = \alpha_k \sum_{\ell=1}^3 \bar{E}_{\ell,(i,2)} \stackrel{\text{DTA}}{=} \alpha_k,$$

where we have used that the matrix  $E^{(0)}$  of Equation (12) is DTA-compatible, so that in particular its columns sum to one. Next, if we impose

$$g_{i+2+(2j-5)n^r+(k-1)(\bar{n}_0+\bar{n}_1)} = f_{4+i+(j-3)n^r+(k-1)\bar{n}_0} - f_{3+i+(j-3)n^r+(k-1)\bar{n}_0} = 0$$

for any  $j \in \{3, \dots, n^s\}$  and  $i \in \{1, \dots, n^r\}$  and

$$g_{i+2+(2j-4)n^r+(k-1)(\bar{n}_0+\bar{n}_1)} = f_{3+i+(j-2)n^r+(k-1)\bar{n}_0} - f_{3+i+(j-3)n^r+(k-1)\bar{n}_0} = 0$$

for any  $j \in \{3, \dots, n^s-1\}$  and  $i \in \{1, \dots, n^r\}$ , we get

$$\begin{cases} f_{4+i+(j-3)n^r+(k-1)\bar{n}_0} = f_{3+i+(j-3)n^r+(k-1)\bar{n}_0} \\ f_{3+i+(j-2)n^r+(k-1)\bar{n}_0} = f_{3+i+(j-3)n^r+(k-1)\bar{n}_0}. \end{cases}$$

Hence, we have that all the coefficients of the form  $f_{\ell+(k-1)\bar{n}_0}$  for a fixed  $k$  are equal to  $\alpha_k$ . However, we further have

$$g_{i+k\bar{n}_1+(k-1)\bar{n}_0} = f_{i+k\bar{n}_0} - f_{i+(k-1)\bar{n}_0} = 0 \Rightarrow f_{i+k\bar{n}_0} = f_{i+(k-1)\bar{n}_0},$$

for  $i \in \{1, \dots, \bar{n}_0\}$ , that is,  $\alpha_{k+1} = \alpha_k = \alpha \in \mathbb{R}$ . We conclude that  $1 = \dim \ker(\text{grad}) = \dim \mathcal{H}^0(\mathfrak{S})$ . Let us now move to the computation of  $\dim \mathcal{H}^3(\mathfrak{S})$ . We show that  $\text{div} : V_2 \rightarrow V_3$  is surjective, so that  $\text{im}(\text{div}) = V_3$  and  $\dim \mathcal{H}^3(\mathfrak{S}) = \dim V_3 - \dim \text{im}(\text{div}) = 0$ . Therefore, given  $m \in V_3$ ,  $m = \mathbf{N}^{(3)} \cdot \mathbf{m}$ , we look for a  $h \in V_2$ ,  $h = \mathbf{N}^{(2)} \cdot \mathbf{h}$ , such that  $\text{div } h = m$ , that is, such that  $D^{(2)}\mathbf{h} = \mathbf{m}$ . By choosing,

```

for  $k = 1, \dots, n^t$ 
   $h_{1+k\bar{n}_2+(k-1)\bar{n}_1} = 0;$ 
   $h_{2+k\bar{n}_2+(k-1)\bar{n}_1} = 0;$ 
  for  $i = 1, \dots, n^r$ 
     $h_{2+i+k\bar{n}_2+(k-1)\bar{n}_1} = 0;$ 
     $h_{2+i+n^r+k\bar{n}_2+(k-1)\bar{n}_1} = -m_{i+(k-1)\bar{n}_2};$ 
  for  $j = 2, \dots, n^s-2$ 
    for  $i = 1, \dots, n^r-1$ 
       $h_{2+i+(2j-2)n^r+k\bar{n}_2+(k-1)\bar{n}_1} = 0;$ 
       $h_{2+i+(2j-1)n^r+k\bar{n}_2+(k-1)\bar{n}_1} = h_{2+i+(2j-3)n^r+k\bar{n}_2+(k-1)\bar{n}_1} - m_{i+(j-1)n^r+(k-1)\bar{n}_2};$ 
       $h_{2+2jn^r+k\bar{n}_2+(k-1)\bar{n}_1} = 0;$ 
       $h_{2+(2j-1)n^r+k\bar{n}_2+(k-1)\bar{n}_1} = h_{2+(2j-2)n^r+k\bar{n}_2+(k-1)\bar{n}_1} - m_{jn^r+(k-1)\bar{n}_2};$ 
    for  $\ell = 1, \dots, \bar{n}_2$ 
       $h_{\ell+(k-1)(\bar{n}_2+\bar{n}_1)} = \beta \in \mathbb{R};$ 

```

one easily can compute that  $D^{(2)}\mathbf{h} = \mathbf{m}$ . Thus  $\dim \mathcal{H}^3(\mathfrak{S}) = 0$ . We move to  $\dim \mathcal{H}^2(\mathfrak{S}) = \dim \ker(\text{div}) - \dim \text{im}(\text{curl})$ . Let us start by calculating  $\dim \ker(\text{div})$ . We have shown that the divergence is surjective, that is,  $\dim \text{im}(\text{div}) = \dim V_3 = n_3 = n^t \bar{n}_2$ . Furthermore, it holds  $\dim \ker(\text{div}) + \dim \text{im}(\text{div}) = \dim V_2 = n_2 = n^t(\bar{n}_1 + \bar{n}_2)$ . Therefore,

$$\dim \ker(\text{div}) = n^t(\bar{n}_1 + \bar{n}_2) - n^t \bar{n}_2 = n^t \bar{n}_1.$$

Now we compute  $\dim \text{im}(\text{curl})$ . With reference to Equation (23), for a fixed  $k$ , let us split the expressions for the entries of  $\mathbf{h}$  into two sets: the relations for the components of the form  $h_{\ell+(k-1)(\bar{n}_1+\bar{n}_2)}$ , for  $\ell = 1, \dots, \bar{n}_2$ , and those for the components  $h_{\ell+k\bar{n}_2+(k-1)\bar{n}_1}$  for  $\ell = 1, \dots, \bar{n}_1$ . Let  $D_1^{(1)}$  be the matrix associated to the first set of relation. By adapting the procedure we used to prove that  $\dim \mathcal{H}^3(\mathfrak{S}) = 0$ , one shows that  $D_1^{(1)}$  has full rank. This is also verified in [35, proof of Theorem 5.10, second cohomology]. Instead, by looking at the second block of equations, one recognize that the associated matrix has the form  $[I_{\bar{n}_1} | D_2^{(1)} | - I_{\bar{n}_1}]$  with  $D_2^{(1)}$  of dimension  $\bar{n}_1 \times \bar{n}_0$ . Indeed, the expressions of  $h_{\ell+k\bar{n}_2+(k-1)\bar{n}_1}$ , for  $\ell = 1, \dots, \bar{n}_1$ , are always of the form  $g_{\ell+(k-1)(\bar{n}_0+\bar{n}_1)}$  plus some linear combination of the coefficients  $g_{q+(k-1)\bar{n}_0+k\bar{n}_1}$ , for  $q = 1, \dots, \bar{n}_0$ , and minus  $g_{\ell+k(\bar{n}_0+\bar{n}_1)}$ . By using the same argument we used to prove that  $\dim \mathcal{H}^1(\mathfrak{S}) = 1$ , one shows that the kernel of  $D_2^{(1)}$  has dimension one. This is also verified in [35, proof of Theorem 5.1, first cohomology].

Hence, by recalling that  $\bar{n}_1 > \bar{n}_0$ , the rank of  $D_2^{(1)}$  is  $\bar{n}_0 - 1$ . Therefore, the rank of  $D^{(1)}$  is  $n^t(\bar{n}_2 + \bar{n}_0 - 1)$ , which is also the dimension of  $\text{im}(\text{curl})$ . We have

$$\begin{aligned}\dim \mathcal{H}^2(\mathfrak{S}) &= \dim \ker(\text{div}) - \dim \text{im}(\text{curl}) \\ &= n^t(\bar{n}_1 - \bar{n}_2 - \bar{n}_0 + 1) \\ &= n^t(2n^r(n^s - 2) + 2 - n^r(n^s - 2) - n^r(n^s - 2) - 3 + 1) = 0.\end{aligned}$$

With the dimensions of  $\mathcal{H}^0(\mathfrak{S})$ ,  $\mathcal{H}^2(\mathfrak{S})$  and  $\mathcal{H}^3(\mathfrak{S})$  at hand, we can easily compute  $\dim \mathcal{H}^1(\mathfrak{S})$  by using the following identity:

$$\dim \mathcal{H}^0(\mathfrak{S}) - \dim \mathcal{H}^1(\mathfrak{S}) + \dim \mathcal{H}^2(\mathfrak{S}) - \dim \mathcal{H}^3(\mathfrak{S}) = \dim V_0 - \dim V_1 + \dim V_2 - \dim V_3.$$

On one hand we have

$$\dim V_0 - \dim V_1 + \dim V_2 - \dim V_3 = n^t(\bar{n}_0 - \bar{n}_0 - \bar{n}_1 + \bar{n}_1 + \bar{n}_2 - \bar{n}_2) = 0,$$

and on the other hand we have proved that

$$\dim \mathcal{H}^0(\mathfrak{S}) = 1, \quad \dim \mathcal{H}^2(\mathfrak{S}) = 0, \quad \dim \mathcal{H}^3(\mathfrak{S}) = 0,$$

so that we must have

$$\dim \mathcal{H}^1(\mathfrak{S}) = 1.$$

□

Since the pushforward operators defined in (8) commute with the differential operators  $\text{grad}$ ,  $\text{curl}$  and  $\text{div}$ , see e.g. [38, Theorem 19.8], the spline complex on  $\Omega^{pol}$

$$\mathfrak{S}^{pol} : 0 \xrightarrow{\text{id}} V_0^{pol} \xrightarrow{\text{grad}} V_1^{pol} \xrightarrow{\text{curl}} V_2^{pol} \xrightarrow{\text{div}} V_3^{pol} \xrightarrow{0} 0,$$

where  $V_i^{pol}$  are the spaces spanned by the functions  $N_\ell^{(i),pol} := \mathcal{F}^i(N_\ell^{(i)})$  for  $i = 1, 2, 3$ , preserves the cohomological structure of the de Rham complex (1), because of Theorem 4.1.

## 5. Conclusions

We have presented a discretization of the de Rham complex (1) on a 3D solid toroidal domain  $\Omega^{pol}$  by means of pushforward restricted spline spaces. Such discretization forms a spline complex preserving the cohomological structure of the continuous complex.

Several extension of this work are possible. Our future research will be concentrated in developing de Rham complex discretizations using locally refinable B-spline spaces, such as LR B-spline spaces or THB-spline spaces, and establishing extraction operators to gain local adaptivity in polar domains. These aspects would then be combined to extend the discretization defined in this paper to spline spaces in which local adaptivity is allowed.

We have decided not to include a section of numerical tests for a matter of length. This will be the content of a forthcoming work in which the discretization proposed here is employed in a GEMPIC method for the numerical solution of a Vlasov-Maxwell system.

## Acknowledgments

I wish to thank Martin Campos Pinto, Stefan Possanner, Espen Sande, Hendrik Speleers and Deepesh Toshniwal for introducing me to this topic and the precious discussions. This work was partially supported by the European Council under the Horizon 2020 Project Energy oriented Centre of Excellence for computing applications - EoCoE, Project ID 676629. The author is member of Gruppo Nazionale per il Calcolo Scientifico, Istituto Nazionale di Alta Matematica.

## References

- [1] D. N. Arnold, *Finite element exterior calculus*, CBMS-NSF Regional Conference Series in Applied Mathematics, vol. 93, Society for Industrial and Applied Mathematics (SIAM), Philadelphia, PA, 2018. MR 3908678
- [2] D. N. Arnold, R. S. Falk, and R. Winther, *Finite element exterior calculus, homological techniques, and applications*, *Acta Numerica* **15** (2006), 1–155.
- [3] ———, *Finite element exterior calculus: from hodge theory to numerical stability*, *Bulletin of the American Mathematical Society* **47** (2010), no. 2, 281–354.
- [4] A. Bock and E. Sonnendrücker, *Finite Element Hodge for spline discrete differential forms. Application to the Vlasov–Poisson system*, *Applied Numerical Mathematics* **79** (2014), 124–136.
- [5] L. Beirão da Veiga, A. Buffa, G. Sangalli, and R. Vázquez, *Analysis-suitable T-splines of arbitrary degree: Definition, linear independence and approximation properties*, *Mathematical Models and Methods in Applied Sciences* **23** (2013), 1979–2003.
- [6] D. Boffi, *Finite element approximation of eigenvalue problems*, *Acta Numerica* **19** (2010), 1–120.
- [7] C. de Boor, *A practical guide to splines*, revised ed., Springer-Verlag, New York, 2001.
- [8] A. Bressan and E. Sande, *Approximation in FEM, DG and IGA: a theoretical comparison*, *Numerische Mathematik* **143** (2019), no. 4, 923–942. MR 4026376
- [9] A. Buffa, J. Rivas, G. Sangalli, and R. Vázquez, *Isogeometric discrete differential forms in three dimensions*, *SIAM Journal on Numerical Analysis* **49** (2011), no. 2, 818–844.
- [10] A. Buffa, G. Sangalli, and R. Vázquez, *Isogeometric analysis in electromagnetics: B-splines approximation*, *Computer Methods in Applied Mechanics and Engineering* **199** (2010), no. 17–20, 1143–1152.
- [11] ———, *Isogeometric methods for computational electromagnetics: B-spline and T-spline discretizations*, *Journal of Computational Physics* **257** (2014), 1291–1320.
- [12] M. Campos Pinto, K. Kormann, and E. Sonnendrücker, *Variational Framework for Structure-Preserving Electromagnetic Particle-In-Cell Methods*, arXiv preprint: <https://arxiv.org/abs/2101.09247> (2021).
- [13] J. Deng, F. Chen, X. Li, C. Hu, W. Tong, Z. Yang, and Y. Feng, *Polynomial splines over hierarchical T-meshes*, *Graphical Models* **70** (2008), 76–86.
- [14] T. Dokken, T. Lyche, and K. F. Pettersen, *Polynomial splines over locally refined box-partitions*, *Computer Aided Geometric Design* **30** (2013), 331–356.
- [15] N. Engleitner and B. Jüttler, *Patchwork B-spline refinement*, *Computer-Aided Design* **90** (2017), 168–179.
- [16] J. A. Evans, M. A. Scott, K. M. Shepherd, D. C. Thomas, and R. Vázquez Hernández, *Hierarchical B-spline complexes of discrete differential forms*, *IMA Journal of Numerical Analysis* **40** (2020), no. 1, 422–473.
- [17] D. R. Forsey and R. H. Bartels, *Hierarchical B-spline refinement*, *ACM Siggraph Computer Graphics* **22** (1988), 205–212.
- [18] J. P. Freidberg, *Plasma Physics and Fusion Energy*, Cambridge University Press, 2008.
- [19] C. Giannelli, B. Jüttler, and H. Speleers, *THB-splines: The truncated basis for hierarchical splines*, *Computer Aided Geometric Design* **29** (2012), 485–498.
- [20] D. Großmann, B. Jüttler, H. Schlusnus, J. Barner, and A. Vuong, *Isogeometric simulation of turbine blades for aircraft engines*, *Computer Aided Geometric Design* **29** (2012), no. 7, 519–531.
- [21] A. Hatcher, *Algebraic Topology*, Cambridge University Press, 2001.
- [22] R. D. Hazeltine and J. D. Meiss, *Plasma Confinement*, Courier Corporation, 2003.
- [23] R. Hiptmair, *Finite elements in computational electromagnetism*, *Acta Numerica* **11** (2002), 237–339.
- [24] F. Holderied, S. Possanner, A. Ratnani, and X. Wang, *Structure-preserving vs. standard particle-in-cell methods: the case of an electron hybrid model*, *Journal of Computational Physics* **402** (2020), 109108.
- [25] T. J. R. Hughes, J. A. Cottrell, and Y. Bazilevs, *Isogeometric analysis: CAD, finite elements, NURBS, exact geometry and mesh refinement*, *Computer Methods in Applied Mechanics and Engineering* **194** (2005), 4135–4195.
- [26] K. A. Johannessen, M. Kumar, and T. Kvamsdal, *Divergence-conforming discretization for Stokes problem on locally refined meshes using LR B-splines*, *Computer Methods in Applied Mechanics and Engineering* **293** (2015), 38–70.
- [27] M. Kraus, K. Kormann, P. J. Morrison, and E. Sonnendrücker, *GEMPIC: geometric electromagnetic particle-in-cell methods*, *Journal of Plasma Physics* **83** (2017), no. 4.
- [28] T. Lyche, C. Manni, and H. Speleers, *Foundations of spline theory: B-splines, spline approximation, and hierarchical refinement*, *Splines and PDEs: From Approximation Theory to Numerical Linear Algebra* (T. Lyche et al., eds.), Lecture Notes in Mathematics, vol. 2219, Springer International Publishing AG, 2018, pp. 1–76.
- [29] C. Manni, F. Pelosi, and M. L. Sampoli, *Isogeometric analysis in advection–diffusion problems: Tension splines approximation*, *Journal of Computational and Applied Mathematics* **236** (2011), no. 4, 511–528.
- [30] C. Manni and H. Speleers, *Standard and non-standard CAGD tools for isogeometric analysis: A tutorial*, *IsoGeometric Analysis: A New Paradigm in the Numerical Approximation of PDEs* (A. Buffa and G. Sangalli, eds.), Lecture Notes in Mathematics, vol. 2161, Springer International Publishing AG, 2016, pp. 1–69.
- [31] L. L. Schumaker, *Spline functions: Basic theory*, third ed., Cambridge University Press, 2007.
- [32] T. W. Sederberg, J. Zheng, A. Bakenov, and A. Nasri, *T-splines and T-NURCCs*, *ACM Transactions on Graphics* **22** (2003), 477–484.
- [33] H. Speleers, *Algorithm 999: Computation of multi-degree B-splines*, *ACM Transactions on Mathematical Software (TOMS)* **45** (2019), no. 4, 1–15.
- [34] H. Speleers and D. Toshniwal, *A general class of C1 smooth rational splines: Application to construction of exact ellipses and ellipsoids*, *Computer-Aided Design* **132** (2021), 102982.

- [35] D. Toshniwal and T. J.R. Hughes, *Isogeometric discrete differential forms: Non-uniform degrees, Bézier extraction, polar splines and flows on surfaces*, Computer Methods in Applied Mechanics and Engineering **376** (2021), 113576.
- [36] D. Toshniwal, H. Speleers, R. R. Hiemstra, and T. J. R. Hughes, *Multi-degree smooth polar splines: A framework for geometric modeling and isogeometric analysis*, Computer Methods in Applied Mechanics and Engineering **316** (2017), 1005–1061.
- [37] D. Toshniwal, H. Speleers, R. R. Hiemstra, C. Manni, and T. J. R. Hughes, *Multi-degree B-splines: Algorithmic computation and properties*, Computer Aided Geometric Design **76** (2020), 101792.
- [38] L.W. Tu, *An Introduction to Manifolds*, Springer, New York, NY, 2011.
- [39] E. Zoni and Y. Güçlü, *Solving hyperbolic-elliptic problems on singular mapped disk-like domains with the method of characteristics and spline finite elements*, Journal of Computational Physics **398** (2019), 108889.